

Yale University

EliScholar – A Digital Platform for Scholarly Publishing at Yale

Yale Medicine Thesis Digital Library

School of Medicine

1996

Photochemotherapy of vascular cells with 8-methoxypsoralen and visible light: a novel approach to the prevention of post-angioplasty restenosis

David Marshall Lee
Yale University

Follow this and additional works at: <http://elischolar.library.yale.edu/ymtdl>

 Part of the [Medicine and Health Sciences Commons](#)

Recommended Citation

Lee, David Marshall, "Photochemotherapy of vascular cells with 8-methoxypsoralen and visible light: a novel approach to the prevention of post-angioplasty restenosis" (1996). *Yale Medicine Thesis Digital Library*. 2835.
<http://elischolar.library.yale.edu/ymtdl/2835>

This Open Access Thesis is brought to you for free and open access by the School of Medicine at EliScholar – A Digital Platform for Scholarly Publishing at Yale. It has been accepted for inclusion in Yale Medicine Thesis Digital Library by an authorized administrator of EliScholar – A Digital Platform for Scholarly Publishing at Yale. For more information, please contact elischolar@yale.edu.

YALE UNIVERSITY LIBRARY



39002086760148

PHOTOCHEMOTHERAPY OF VASCULAR CELLS WITH
8-METHOXYPsorALEN AND VISIBLE LIGHT;
A NOVEL APPROACH TO THE PREVENTION OF
POST-ANGIOPLASTY RESTENOSIS

DAVID MARSHALL LEE

Yale University

1996

YALE
UNIVERSITY



CUSHING/WHITNEY
MEDICAL LIBRARY


Permission to photocopy or microfilm processing of this thesis for the purpose of individual scholarly consultation or reference is hereby granted by the author. This permission is not to be interpreted as affecting publication of this work or otherwise placing it in the public domain, and the author reserves all rights of ownership guaranteed under common law protection of unpublished manuscripts.



Signature of Author

3/28/96

Date



Digitized by the Internet Archive
in 2017 with funding from
The National Endowment for the Humanities and the Arcadia Fund

PHOTOCHEMOTHERAPY OF VASCULAR CELLS WITH 8-METHOXYPSORALEN AND VISIBLE LIGHT: A NOVEL APPROACH TO THE PREVENTION OF POST-ANGIOPLASTY RESTENOSIS

A Thesis Submitted to the
Yale University School of Medicine
in Partial Fulfillment of the Requirements for the
Degree of Doctor of Medicine

by

David Marshall Lee

1996

YALE MEDICAL LIBRARY

AUG 14 1996

MED
T113
+Y12
6398

PHOTOCHEMOTHERAPY OF VASCULAR CELLS WITH 8-METHOXYPsorALEN AND VISIBLE LIGHT: A NOVEL APPROACH TO THE PREVENTION OF POST-ANGIOPLASTY RESTENOSIS

David M. Lee, Francis P. Gasparro, and Bauer E. Sumpio. Section of Vascular Surgery, Department of Surgery, Yale University, School of Medicine, New Haven, CT.

The purpose of the present study was to evaluate the effects of photochemotherapy with 8-methoxypsoralen (8-MOP) and visible light (447 nm) on vascular cells *in vitro*. It was hypothesized that this treatment regimen could selectively inhibit smooth muscle cell proliferation and might thus represent a novel approach to the prevention of post-angioplasty restenosis.

Bovine aortic smooth muscle cells (SMC) and endothelial cells (EC) were cultured in cell wells, incubated with 1, 20, or 50 $\mu\text{g}/\text{mL}$ 8-MOP, and then exposed to 12.0 J/cm^2 447 nm visible light. Control cells were wrapped with aluminum foil so as to prevent 8-MOP photoactivation. Studies were then undertaken to ascertain the effects of these treatment regimens on SMC and EC proliferation, migration, morphology, size, and photoadduct formation.

Experiments on SMC proliferation revealed no significant effect at 1 $\mu\text{g}/\text{mL}$ 8-MOP, while 20 $\mu\text{g}/\text{mL}$ produced a transient, reversible inhibition, and 50 $\mu\text{g}/\text{mL}$ resulted in cell death. Experiments on EC proliferation also revealed no significant effect at 1 $\mu\text{g}/\text{mL}$ 8-MOP; however, a transient, reversible inhibition was seen at both 20 and 50 $\mu\text{g}/\text{mL}$ 8-MOP. Further experimentation revealed that photoactivated 8-MOP does not inhibit cell migration. Morphology studies demonstrated both size and phenotype changes induced by higher dosages (20 and 50 $\mu\text{g}/\text{mL}$) of 8-MOP. Cell size measurements corroborated the cell enlargement observed in the morphology studies. Followed over time, EC revealed a return to baseline sizes while SMC remained enlarged. Finally, studies on photoadduct formation revealed the formation of comparable numbers and types of photoadducts between SMC and EC.

These experiments demonstrate that while 8-MOP photoactivated with 447 nm visible light can reversibly inhibit the proliferation of both SMC and EC in a dose-dependent fashion, SMC are more sensitive to the treatments than EC. The rapidly reversible inhibition observed in EC proliferation bears clinical significance, as previous studies have demonstrated that an intact endothelium contributes to the

inhibition of SMC proliferation. As SMC proliferation constitutes a major mechanism by which restenosis after angioplasty occurs, the results of this study suggest that photochemotherapy with 8-MOP and visible light may represent a novel approach to the prevention of post-angioplasty restenosis.

Acknowledgements

I would like to begin by thanking Dr. Bauer Sumpio for his guidance and mentorship over the past few years. The time I have spent working in his lab and the things I have learned through my experiences there account for a substantial portion of my medical school training. Since the time I first set foot in his office, his model of true excellence in his own work has not stopped being a source of inspiration to me.

I also want to thank the people in the lab who have made my time working on this project a most enjoyable one—to Dr. Guangdi Li, who taught me the finer points of cell culturing, and to Drs. Wei Du and Ira Mills, backbones of the lab who were always willing to lend a helping hand.

A special thanks to Dr. Frank Gasparro for the time he invested in me and my work. His unparalleled expertise in the photobiology of psoralens and computer wizardry were invaluable in the development and completion of this project.

Thanks also to my brothers and sisters in the Yale Health Professionals Christian Fellowship. I have appreciated their prayers and encouragement throughout the years.

I cannot begin to express my gratitude to my parents and to my wife, who have persevered with me through my journey toward becoming a medical doctor. Their unconditional love and support have brought out the best in me and have been a source of immeasurable joy and strength.

Finally, I would like to give thanks and glory to God, who has granted us both the curiosity and the minds to explore the wonders of his creation. . .

Table of Contents

| | |
|--|-----------|
| 1. PERCUTANEOUS TRANSLUMINAL CORONARY ANGIOPLASTY (PTCA) | 3 |
| The Normal Coronary Artery | 3 |
| The Diseased Coronary Artery: Atherosclerosis | 4 |
| Advances in PTCA | 7 |
| 2. RESTENOSIS: THE ACHILLES' HEEL OF PTCA | 11 |
| Restenosis: The Problem | 11 |
| Restenosis: The Economic Impact | 12 |
| Restenosis: Temporal Considerations | 13 |
| Early Restenosis: Thrombosis, Recoil, and Vasoconstriction | 13 |
| Late Restenosis: Vascular Wound Healing | 14 |
| Phase I of Vascular Wound Healing: Inflammation | 14 |
| Phase II of Vascular Wound Healing: Granulation | 15 |
| Phase III of Vascular Wound Healing: Matrix Formation | 17 |
| 3. PHARMACOLOGIC APPROACHES TO THE PREVENTION OF RESTENOSIS | 19 |
| Antiplatelet Agents | 21 |
| Antithrombotic Agents | 23 |
| Lipid-lowering Agents | 24 |
| Antispasmodic Agents | 25 |
| Antineoplastic Agents | 25 |
| Antiproliferative Agents | 26 |
| 4. PHOTOCHEMOTHERAPY WITH 8-MOP AND VISIBLE LIGHT | 28 |
| Photochemotherapy | 28 |
| 8-Methoxypsoralen (8-MOP) | 29 |

| | |
|--------------------------------|-----------|
| | 2 |
| 5. STATEMENT OF PURPOSE | 37 |
| 6. EXPERIMENTAL METHODS | 39 |
| Cell Culture | 39 |
| Chemicals | 40 |
| Experimental Protocol | 40 |
| Cell Counts | 41 |
| Cell Migration | 41 |
| Cell Morphology | 42 |
| Cell Size | 43 |
| Photoadduct Formation | 43 |
| Statistical Analysis | 44 |
| 7. RESULTS | 45 |
| SMC Proliferation | 45 |
| EC Proliferation | 50 |
| Cell Migration | 55 |
| Cell Morphology | 56 |
| Cell Size | 60 |
| Photoadduct Formation | 63 |
| 8. DISCUSSION | 64 |
| Discussion of Results | 64 |
| Potential Future Experiments | 67 |
| Significance of Results | 69 |
| 9. CONCLUSION | 72 |
| 10. REFERENCES | 73 |

1. Percutaneous Transluminal Coronary Angioplasty (PTCA)

The Normal Coronary Artery

Coronary artery disease remains the number one cause of morbidity and mortality in the Western world. It results from the development of atherosclerotic lesions in the coronary arteries, or vessels which supply the heart. The anatomy of the normal coronary artery is no different from that of other medium-sized arteries in the human body; namely, the vessel wall possesses three layers—an intima, media, and adventitia.

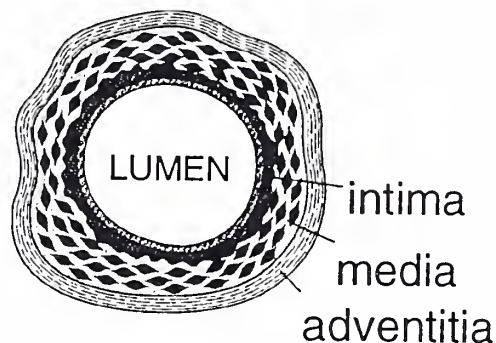


Figure 1-1. Schematic representation of the three layers of the coronary artery. Figure modified from Libby, 1992.

The intima is the layer closest to the lumen of the vessel and is primarily comprised of a monolayer of endothelial cells (EC) lining an underlying coat of connective tissue. It is separated from the media by a fenestrated membrane through which the smooth muscle cells (SMC) of the media can migrate, called the internal elastic membrane. The media, or muscular layer, of the artery forms the major structural support for the vessel and consists of several layers of SMC separated by compact, fenestrated layers of elastic tissue. A condensation of this elastic tissue at the perimeter of the media forms the external elastic membrane, which separates the media from the outermost layer of the artery, the adventitia. A poorly defined layer of connective tissue, the adventitia contains fibroblasts, elastic fibers, nerve fibers, and small nutrient vessels known as *vasa vasora*. These thin-walled vessels serve as the blood supply to the adventitial layer and to the outer portion of the media.

The Diseased Coronary Artery: Atherosclerosis

The hypothesis that an injury to the endothelium is the precipitating event in the development of atherosclerosis was first formally proposed in 1973 by Ross and Glomset (Ross and Glomset, 1973) and is still widely held today.

Commonly cited potential causes of injury include diabetes, hypertension, tobacco, radiation, and hyperlipidemia. Over the past two decades, our understanding of the pathogenesis of atherosclerosis has substantially increased and been refined by accumulating observations on the various cell types and molecules involved in atherogenesis.

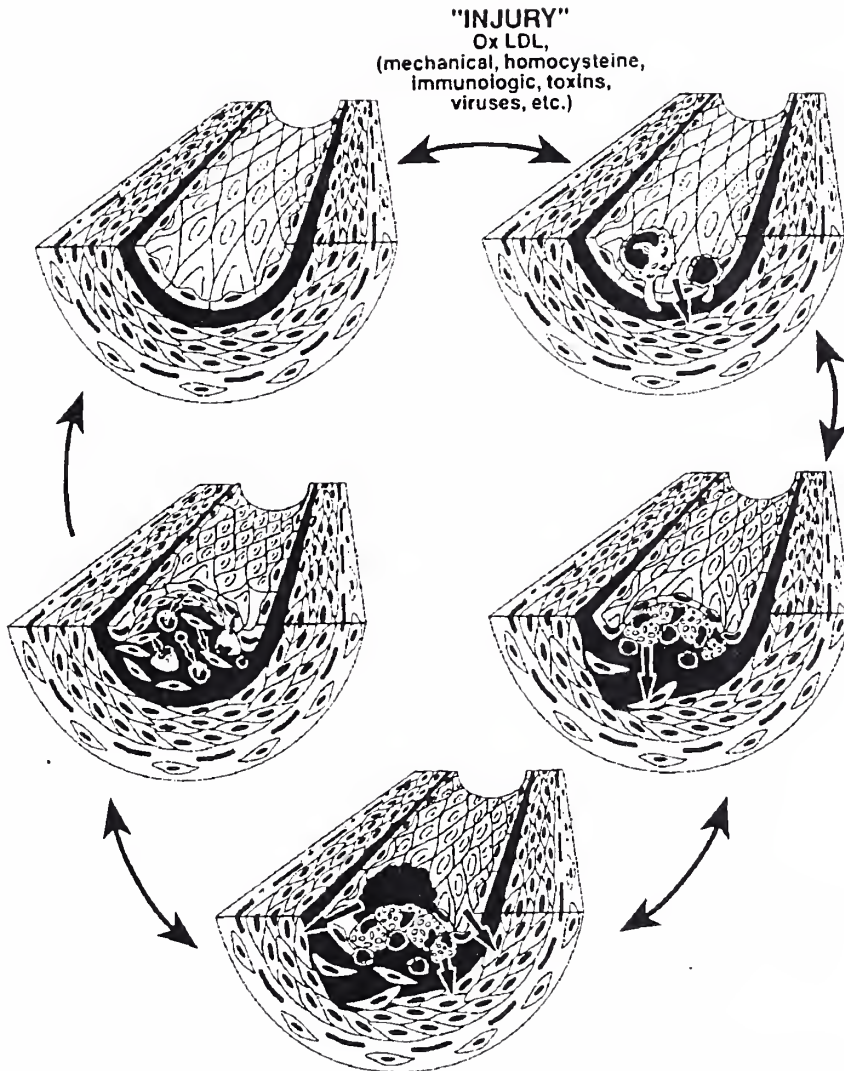


Figure 1-2. Schematic representation of the response-to-injury hypothesis of atherosclerosis. Several different sources of injury to the endothelium can lead to the formation of a fatty streak, which can ultimately progress to a fibrous plaque. Each of the stages of lesion formation is potentially reversible. Thus, lesion regression can occur if the injurious agents are removed or when protective factors intervene to reverse the inflammatory and fibroproliferative processes. Figure taken from Ross, 1993.

The earliest recognizable lesion of atherosclerosis is the "fatty streak," which consists of an aggregation of lipid-laden macrophages, or foam cells, in the intima.

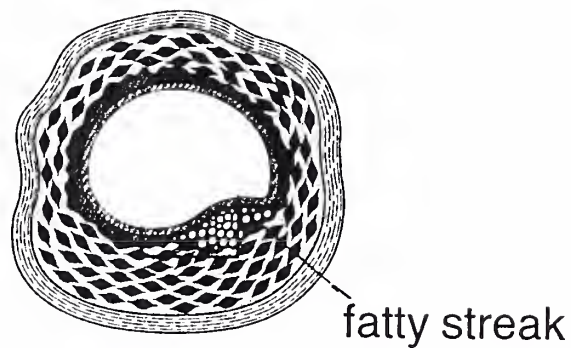


Figure 1-3. Schematic representation of a fatty streak. Figure modified from Libby, 1992.

Presumably, this lesion progresses as SMC migrate from the media into the intima and elaborate a connective tissue matrix. This results in the projection of the lesion, now termed a “fibrous plaque,” into the arterial lumen. Eventually, extracellular cholesterol, calcium deposits, and necrotic cellular debris accumulate with the foam cells at the core of the lesion. Finally, the plaque is covered over by a dense fibrous cap made of connective tissue embedded with SMC (Ross, 1993; Lovqvist et al., 1993).

It is important to note that the majority of atherosclerotic lesions are eccentric rather than concentric; that is, the majority of lesions involve only a portion of the arterial circumference rather than the entire circumference (Waller, 1985).

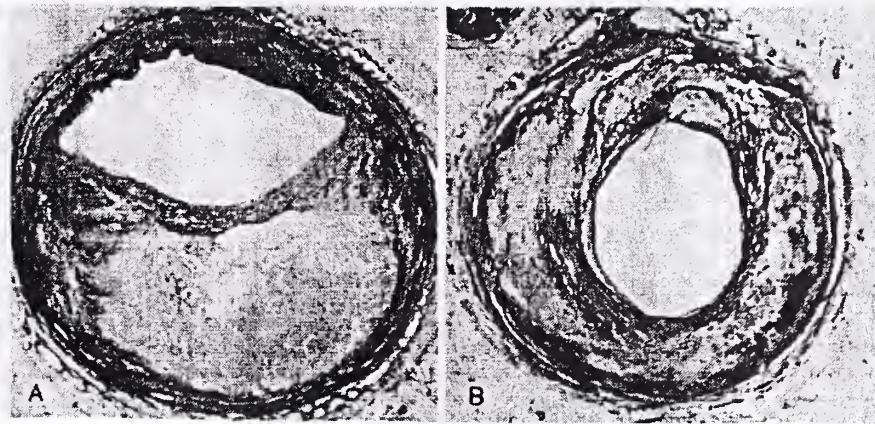


Figure 1-4. Atherosclerotic lesions in coronary arteries. A: an eccentric lesion (bottom) with disease-free segment (top). B: markedly calcified concentric plaque. Figure taken from Edwards, 1995.

An increase in size in one of these fibrous plaques causes arterial stenosis, or a narrowing of the arterial luminal cross-sectional area. This, in turn, results in an increased resistance to blood flow. When present to a sufficient degree in coronary arteries, these stenotic lesions may cause symptoms of stable angina. Fissures or ruptures in the fibrous cap, on the other hand, may result in hemorrhage into the plaque, thrombosis, and acute arterial occlusion. This latter sequence is responsible for the majority of sudden deaths caused by myocardial infarcts (Davies and Thomas, 1984).

Advances in PTCA

Non-pharmacologic therapies for symptomatic coronary artery disease include coronary artery bypass grafting (CABG) and percutaneous transluminal coronary angioplasty

(PTCA). Whereas surgical bypass is the standard of care in cases of left main coronary artery disease, triple vessel disease with compromised ventricular function, and anginal symptoms resistant to medical therapy, PTCA has been established as a significant option in the treatment of patients with coronary artery disease. Up to 50% of all patients requiring revascularization choose this considerably less invasive procedure as an alternative to bypass surgery (Ip et al., 1990).

Balloon angioplasty, the most common form of PTCA, involves the passage of a balloon along a guide wire to a site of arterial stenosis. Subsequent dilation of the balloon typically produces a stretching of plaque-free wall and fracturing or “cracking” of plaque and hence a widened lumen diameter.

First introduced in September 1977 by Andreas Gruentzig (Gruentzig et al., 1979), PTCA was initially received with skepticism. Today, it has become the treatment of choice for many patients with coronary artery disease who require revascularization (Lange et al., 1993).

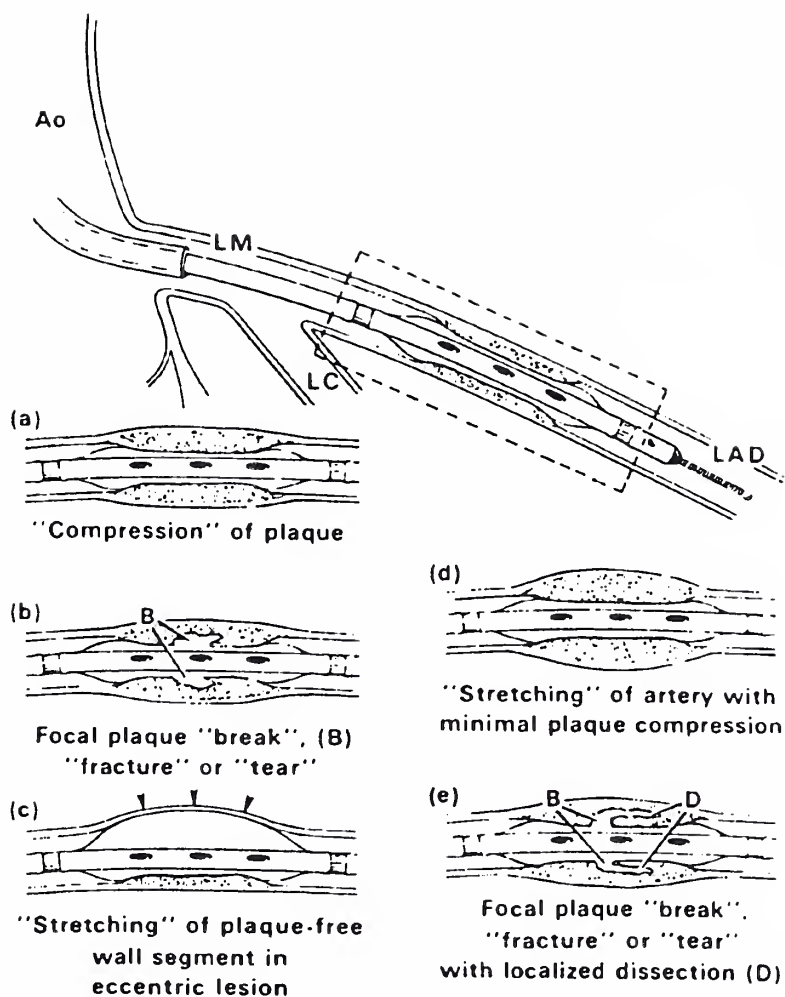


Figure 1-5. Mechanisms by which balloon angioplasty can induce revascularization. Ao = aorta; LAD = left anterior descending; LC = left circumflex; LM = left main coronary artery. Figure taken from Waller, 1985.

Formerly limited to cases involving simple single-vessel disease, PTCA has now been applied in cases involving complex stenoses, occluded arteries, multivessel disease,

saphenous vein grafts, and acute myocardial infarction (Lange et al, 1993). Despite its application in increasingly complex cases, improvements in technique and advances in catheter technology have continued to improve the success rate of this procedure. With a primary success rate of nearly 95% (Hermans et al., 1991), over 350,000 coronary angioplasty procedures are being performed each year in the United States (Faxon and Currier, 1995). The long-term efficacy of this minimally invasive treatment modality, however, continues to be severely limited by the problem of post-angioplasty restenosis.

2. Restenosis: The Achilles' Heel of PTCA

Restenosis: The Problem

Restenosis is the re-narrowing of a segment of artery formerly subjected to a percutaneous intervention such as balloon angioplasty.

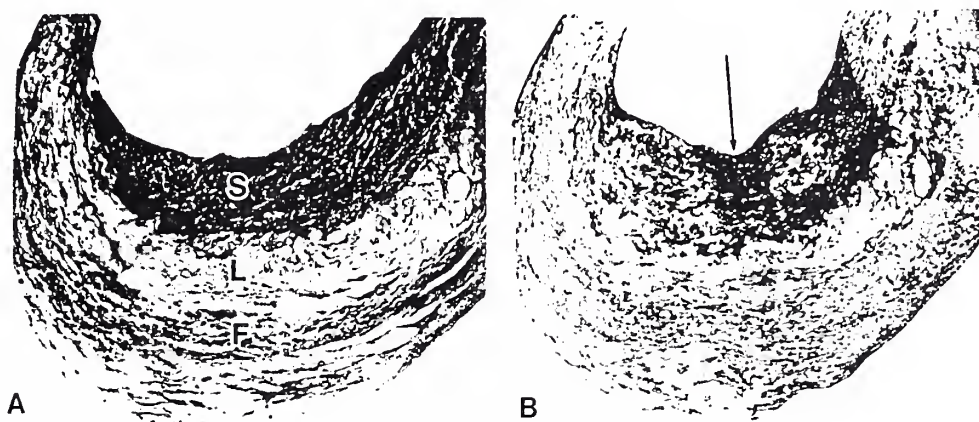


Figure 2-1. Atherectomy specimen from femoral artery of a patient who developed restenosis after balloon angioplasty. A: S = zone of SMC proliferation; L = acellular lipid core of the plaque; F = deeper fibrous region. B: arrow pointing to region of intense SMC proliferation. Figure taken from Forrester et al., 1991.

Traditionally, restenosis rates have been quoted to range anywhere from 5% to 50%. A more contemporary view of restenosis, however, holds that it actually occurs in all patients who undergo PTCA (Ip et al., 1991; Lovqvist et al., 1993) and that its clinical significance is merely a matter of extent. A recent angiographic follow-up study which revealed a near-gaussian distribution of luminal narrowing following PTCA (Rensing,

1992) supports this notion that restenosis is a continuous process rather than “all or nothing” phenomenon.

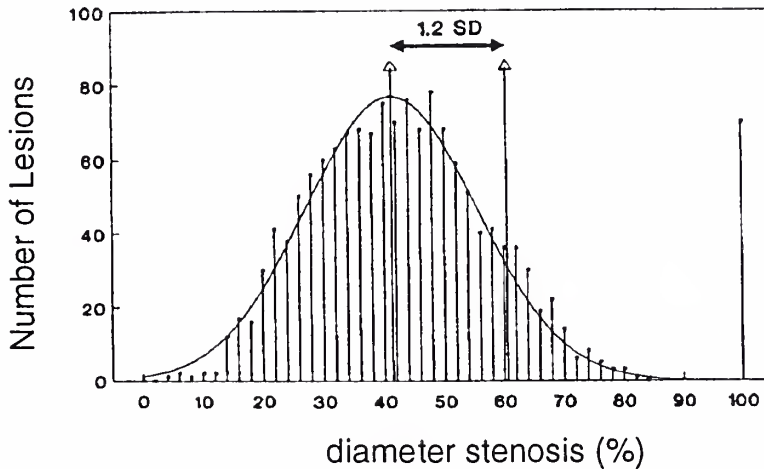


Figure 2-2. Histogram of per cent diameter stenosis seen at follow-up angiography in 1,445 lesions. The curve superimposed on the histogram represents the theoretic gaussian distribution curve. Figure modified from Rensing et al., 1992.

Restenosis: The Economic Impact

A major cause of morbidity, restenosis manifests most frequently as recurrent symptomatic angina requiring additional revascularization procedures. A treatment capable of reducing the risk of restenosis by 25% would average a calculated savings of \$1400 per patient in hospital, procedural, and professional fees, while a risk reduction of 33% would save \$2000 per patient (Califf, 1995). Accordingly, the magnitude of the problem of restenosis, in terms of health care costs, exceeds one billion dollars annually in the United States alone (Faxon and Currier, 1995).

Restenosis: Temporal Considerations

Restenosis can be classified as early or late depending on the histopathology of the restenosed arterial wall. Pathologic examinations of restenosis sites from patients who died after successful PTCA have revealed two types of lesion: those with only fibrous atheromatous plaques resembling the primary plaque and those with substantial intimal thickening secondary to SMC proliferation and matrix elaboration (Waller et al., 1991). The former is associated with early restenosis and the latter with late restenosis (Lovqvist et al., 1993; Lange et al., 1993).

Early Restenosis: Thrombosis, Recoil, and Vasoconstriction

Early restenosis occurs within days of PTCA. One mechanism by which it is thought to occur involves thrombus formation. The mechanical disruption of the intima caused by balloon angioplasty results in endothelial denudation of the plaque. This, in turn, promotes platelet aggregation and may precipitate the acute formation of a thrombus (Lovqvist et al., 1993).

An alternative mechanism in the pathogenesis of early restenosis involves the relaxation and vasoconstriction of stretched plaque-free portions of artery. A quantitative angiographic assessment of coronary arteries before, during, and immediately after angioplasty revealed that nearly 50% of the maximal luminal cross-sectional area achieved during PTCA is lost shortly after balloon deflation, and this presumably due to elastic recoil (Rensing et al., 1990). Additionally, the arterial vasoconstriction frequently observed at the site of coronary angioplasty (Bertrand et al., 1989) may be attributable

both to a decrease in vasodilators produced by disrupted endothelial cells and to an increase in vasoconstrictors released by platelets (Lange et al., 1993).

Late Restenosis: Vascular Wound Healing

A complete understanding of the biologic mechanisms involved in the pathogenesis of late restenosis has yet to be established; however, several of the mechanisms which are involved in the process have been elucidated. Balloon angioplasty is known to inflict substantial injury on the intima and media of the vessel wall, and it is becoming increasingly accepted that the process of restenosis can be understood as a “wound healing” response to such injury (Serruys et al., 1988; Forrester et al., 1991; Ip et al., 1991; Clinton and Libby, 1992; Faxon and Currier, 1995). The ultimate result of this wound healing response is the formation of a neointima consisting of an increased mass of smooth muscle cells (SMC) scattered through a loose extracellular matrix. This neointima formation is the mechanism by which late restenosis occurs.

Phase I of Vascular Wound Healing: Inflammation

It has been suggested that the process of late restenosis occurs over a series of three phases: inflammation, granulation, and matrix formation (Forrester et al., 1991). The first phase, known as the inflammation phase, occurs almost immediately after the injury and continues for several days. It begins with platelet aggregation at the site of the wound surface and thrombus formation (Wilentz et al., 1991). As the blood and soluble serum fibronectin coagulate to form an extracellular matrix, the activated platelets release platelet-derived growth factor (PDGF), a major stimulus of SMC migration and

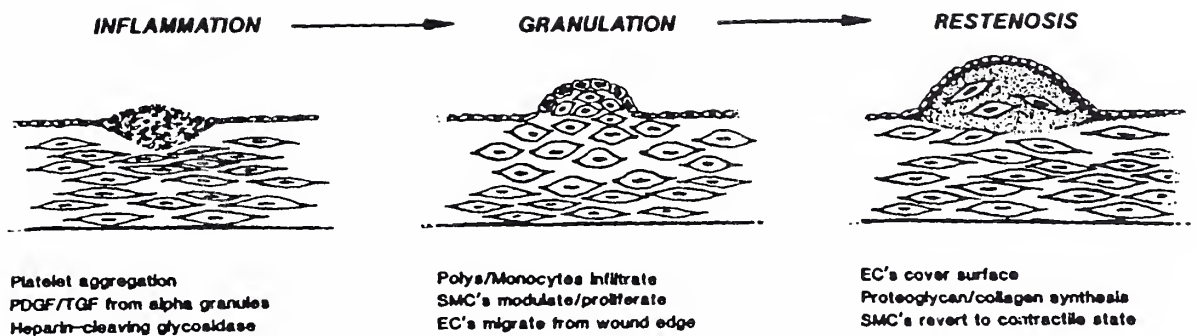


Figure 2-3. Hypothetical schema for late restenosis. PDGF = platelet-derived growth factor; TGF = transforming growth factor; Polys = polymorphonuclear cells; SMC = smooth muscle cells; EC = endothelial cells. Figure taken from Forrester et al., 1991.

proliferation, and other mitogenic factors, including epidermal growth factor and beta transforming growth factor (Ip et al., 1991). Monocytes soon collect in the area of injury and release additional growth factors (Forrester et al., 1991). Meanwhile aggregated mononuclear lymphocytes contribute cytokines such as tumor necrosis factor, interleukins, and beta transforming growth factor (Ip et al., 1991). The release of these various cytokines and growth factors results in a local milieu capable of stimulating SMC migration and proliferation and extracellular matrix production. Hence, the stage is set for the next phase of restenosis.

Phase II of Vascular Wound Healing: Granulation

The second phase of restenosis, called the granulation phase (Forrester et al., 1991), lasts approximately one week and primarily involves the migration and proliferation of SMC. Initial SMC proliferation is reported to begin as early as 24 to 48 hours following

vascular injury. Two to three days later, SMC begin to migrate to the intima, where they may continue to proliferate (Lange et al., 1993).

The stimulus for SMC migration and proliferation is multifactorial and, in addition to the presence of growth factors described above, involves endothelial disruption and direct damage to the EC and SMC. The intimal disruption associated with PTCA may promote SMC proliferation by removing the growth-inhibitory influences exerted by an intact endothelium (Ip et al., 1991). Confluent EC have been observed to secrete heparin-like glycosaminoglycans (Castellot et al., 1981), while exogenous heparin has been shown to inhibit SMC proliferation in injured arteries (Clowes and Karnowsky, 1977). Put together, these facts suggest that a functionally intact endothelium can inhibit SMC growth (Ip et al., 1990). Hence, endothelial disruption, in addition to the presence of mitogens and growth factors, may promote SMC proliferation.

Damaged EC and SMC may also contribute to the mitogenic activity of healthy SMC. EC have the ability to secrete at least two major mitogens, one of which closely resembles PDGF. Meanwhile, SMC also possess the ability to produce a PDGF-like protein. It has been reported that dying EC can produce greater than six times the amount of growth factors produced by healthy EC. Likewise, SMC isolated from injured segments of artery have been found to produce PDGF-like substances on the order of ten times that released by SMC from uninjured segments (Ip et al., 1990).

It should be noted that the SMC proliferating at the site of arterial injury are of the synthetic, rather than contractile, phenotype. Contractile-phenotype SMC predominate in

healthy adult vascular media, whereas synthetic-phenotype SMC exist in young developing arteries. Synthetic-phenotype SMC are closely related to fibroblasts and possess abundant synthetic organelles including free ribosomes, rough endoplasmic reticula, and Golgi apparatus (Forrester et al., 1991). They are “synthetic” in the sense that they synthesize and secrete large quantities of extracellular matrix collagen, elastin, and proteoglycans. These synthetic SMC are the primary cell type involved in the final phase of the wound-healing response, the matrix formation phase.

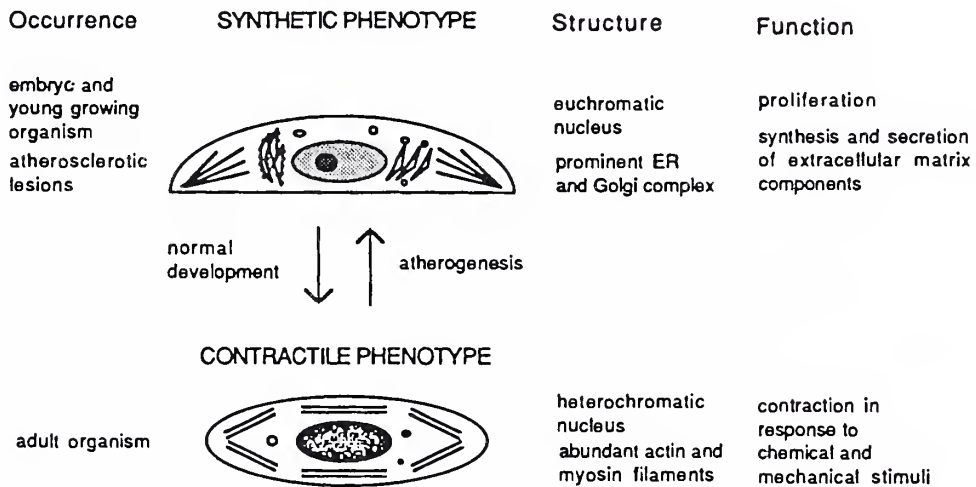


Figure 2-4. Diagrams comparing contractile- and synthetic-phenotype SMC. ER = endoplasmic reticulum. Figure taken from Thyberg et al., 1990.

Phase III of Vascular Wound Healing: Matrix Formation

The matrix formation phase of restenosis primarily involves extracellular matrix deposition and remodeling. As the surface of the site of injury becomes covered with a layer of cells, the SMC which have migrated to the wound area slow their proliferation

and begin to deposit large amounts of proteoglycan, most notably chondroitin sulfate and dermatan sulfate. Neighboring EC also contribute heparin sulfate proteoglycan to the extracellular matrix deposit. Over a course of months, these proteoglycans become replaced by large bundles of type I collagen and elastin (Forrester et al., 1991). This replacement of proteoglycan by collagen and elastin constitutes remodeling and signifies the completion of the final phase of restenosis.

3. Pharmacologic Approaches to the Prevention of Restenosis

The amount of time it takes to advance through the three phases of restenosis described in the previous chapter is somewhat variable, but the entire process of neointima formation is reported to be largely complete by 90 to 120 days (Forrester et al., 1991).

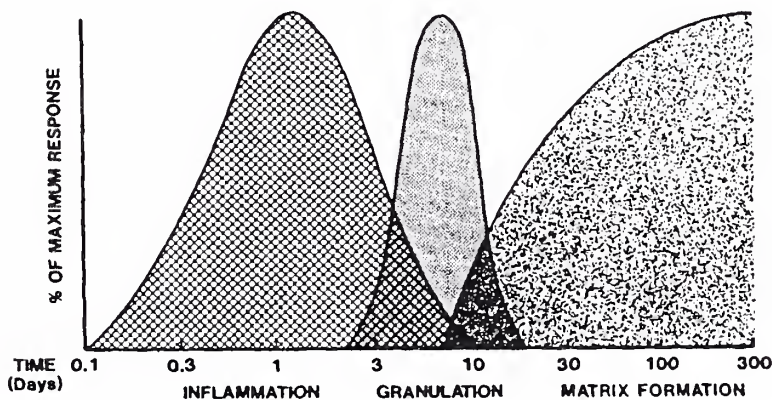


Figure 3-1. Time course for the three phases of wound healing. Figure modified from Forrester et al., 1991.

The fact that this process occurs over a multiplicity of steps suggests that the problem of restenosis can potentially be addressed at a number of levels. Accordingly, a variety of drugs aimed at reducing platelet adhesion, thrombosis, fibrin formation, growth factor expression, and SMC proliferation have been suggested (Ip et al., 1990; Hermans et al., 1991).

Multiple classes of drug have been studied in experiments aimed at reducing or preventing post-angioplasty restenosis. These include antiplatelet agents, antithrombotic agents, lipid-lowering agents, antispasmodic agents, antineoplastic agents, and antiproliferative agents. It should be noted that while many approaches have successfully inhibited restenosis in rat or rabbit models, none have proven effective in pig or primate models, and none have been successful at preventing restenosis in human clinical trials (Wilcox et al., 1993).

Pharmacologic Approaches to Post-angioplasty Restenosis

| | |
|---|---|
| aspirin | dipyridamole |
| ticlopidine | prostacyclin |
| thromboxane A2 inhibitors | monoclonal antibodies to GP IIb/IIIa |
| heparin | low molecular weight heparin |
| warfarin | hirudin |
| cholesterol synthesis inhibitors | fish oils |
| nifedipine | diltiazem |
| vincristine | actinomycin D |
| methotrexate colchicine | glucocorticoids |
| cilazapril | angiopeptin |
| trapidil | |

Table 3-1. Summary of some of the different agents used in experiments designed to reduce or prevent restenosis after angioplasty.

Antiplatelet Agents

The antiplatelet agents studied have included aspirin, dipyridamole, ticlopidine, prostacyclin, thromboxane A2 inhibitors, and monoclonal antibodies to the platelet receptor GP IIb/IIIa. The theoretical basis for their use in strategies designed to prevent post-angioplasty restenosis is founded on the premise that inhibition of platelet deposition may reduce SMC exposure to PDGF and other growth factors which can stimulate neointima formation. One study examining the role of platelets in post-angioplasty restenosis revealed that thrombocytopenic rabbits experienced a marked reduction in intimal thickening following balloon-induced arterial injury (Friedman et al., 1977).

Aspirin, dipyridamole, and ticlopidine. Aspirin inhibits platelet aggregation by irreversibly acetylating the enzyme cyclooxygenase, thereby suppressing the synthesis of proaggregatory thromboxane A2. Dipyridamole acts by increasing intracellular levels of cyclic AMP via the inhibition of cyclic nucleotide phosphodiesterase, which in turn may potentiate prostacyclin's ability to antagonize platelet adhesion to thrombogenic surfaces. While the combination of aspirin and dipyridamole has been shown to decrease the incidence of acute complications both during and after PTCA, it has proven ineffective in preventing restenosis (Schwartz et al., 1988; Chesebro et al., 1989). Ticlopidine, which acts by altering the platelet membrane such that ADP-induced exposure of the fibrinogen binding site on platelet glycoprotein IIb/IIIa is prevented, is another platelet inhibitor. Studies using this agent have also failed to demonstrate beneficial effects on restenosis (White et al., 1987).

Prostacyclin and ciprostone. Prostacyclin is a naturally occurring arachidonic acid metabolite which possesses both platelet inhibitory and vasodilatory properties.

Administration of prostacyclin shortly before PTCA and continued for 48 hours after failed to reduce the incidence of restenosis (Knudtson et al., 1990). Likewise, short-term administration of ciprostone, a prostacyclin analogue, failed to affect the incidence of angiographically-determined restenosis, although some clinical benefit was noted (Raizner, 1988).

Thromboxane A2 inhibitors. In addition to its proaggregatory effects on platelets, thromboxane A2 has been shown to have a mitogenic effect on vascular SMC (Hanasaki et al., 1990). Thromboxane A2 inhibitors work by blocking the formation of thromboxane and redirecting the metabolism of prostaglandin endoperoxides toward prostacyclin synthesis. A small, promising study suggested that thromboxane A2 synthetase inhibitors might prove beneficial in preventing restenosis (Yabe et al., 1989). However, a subsequent randomized, double-blind, placebo-controlled trial involving blockade of the thromboxane A2-receptor revealed no reduction in incidence of restenosis (Serruys et al., 1991).

Antibodies to GP IIb/IIIa. Glycoprotein IIb/IIIa is a platelet membrane receptor which plays an important role in the adhesion of platelets to the vessel wall (Ip et al., 1990). It is also involved in the binding of fibrinogen to platelets (Lovqvist et al., 1993). While the administration of monoclonal antibodies to GP IIb/IIIa has been found to prevent acute thrombosis in the canine model (Bates et al., 1988), its effectiveness in preventing post-

angioplasty restenosis in humans has not been demonstrated and is currently being evaluated in ongoing clinical trials (Faxon and Currier, 1995).

Antithrombotic Agents

The antithrombotic agents studied have included heparin, low molecular weight heparin, warfarin, and hirudin. The theoretical basis for their use in strategies designed to prevent post-angioplasty restenosis involves the role that thrombus formation plays in both early and late restenosis. As described in the previous chapter, acute thrombosis represents a mechanism by which early restenosis may occur. Moreover, during thrombosis, thrombin may become incorporated into both the arterial extracellular matrix and the thrombus itself and can be gradually released during fibrinolysis. As thrombin has been demonstrated to have mitogenic activity for SMC (Ip et al., 1991), it may thus play an important role in the long-term stimulation of SMC proliferation.

Heparin. As mentioned previously, heparin has been found to inhibit SMC proliferation *in vivo* (Clowes and Karnowsky, 1977). While standardly administered to patients during and in the hours following PTCA to prevent acute coronary thrombosis (Lange et al., 1993), heparin given for 18 to 24 hours has failed to demonstrate a reduction in incidence of restenosis (Ellis et al., 1989).

Low molecular weight heparin. Low molecular weight heparin was found to reduce restenosis after angioplasty in the rabbit model (Pow et al., 1989). However, one-month treatments with subcutaneous low molecular weight heparin in a double-blind randomized trial have proven ineffective at preventing restenosis (Faxon et al., 1992).

Warfarin. Warfarin is a vitamin K antagonist which inhibits coagulation and thrombin formation. Several small clinical trials evaluating the effects of warfarin given after angioplasty have failed to demonstrate a decrease in restenosis (Franklin, 1993).

Hirudin. Hirudin is a potent antithrombotic agent which has proven to be more effective than heparin in preventing thrombosis in animal models (Lovqvist et al., 1993). Its effectiveness in preventing post-angioplasty restenosis has yet to be demonstrated (Faxon and Currier, 1995).

Lipid-lowering Agents

The lipid-lowering agents studied have included cholesterol synthesis inhibitors and fish oils. The theoretical advantage of a reduction in lipids in the prevention of post-angioplasty restenosis is based on the paradigm of accelerated atherosclerosis as a model for restenosis (Ip et al., 1990).

Lovastatin. Lovastatin, a cholesterol synthesis inhibitor with antiproliferative properties (Gellman et al., 1991), had previously shown promise in its ability to reduce restenosis in a randomized clinical trial (Sahni et al., 1989). A recently-completed large double-blind controlled trial, however, casts doubt on its effectiveness at preventing post-angioplasty restenosis (Weintraub et al., 1992).

Fish oils. Fish oils, rich in omega-3 fatty acids, are known to decrease LDL cholesterol while simultaneously increasing HDL cholesterol. It has been suggested that fish oils may reduce SMC proliferation by inhibiting EC production of a PDGF-like protein (Fox and

DiCorleto, 1988). Several randomized clinical trials designed to evaluate the effects of fish oils on restenosis have been performed and offer conflicting results. While nearly half of the clinical trials to date involving fish oils have demonstrated some beneficial reduction in restenosis (Franklin et al., 1993), a recently-completed randomized controlled clinical study involving large doses of omega-3 fatty acids with a minimum of two weeks pretreatment revealed that fish oils were not effective at inhibiting restenosis (Faxon and Currier, 1995).

Antispasmodic Agents

The antispasmodic agents studied have included the calcium channel blockers nifedipine and diltiazem. The theoretical basis for their application in strategies designed to prevent post-angioplasty restenosis involves the contribution of coronary vasoconstriction and vasospasm to the process of early restenosis.

Nifedipine and diltiazem. Despite some promising results in animal models, clinical trials in humans have shown that neither nifedipine nor diltiazem demonstrates a beneficial effect on restenosis (Whitworth et al., 1986; O'Keefe et al., 1991).

Antineoplastic Agents

The antineoplastic agents studied have included vincristine, actinomycin D, and methotrexate. The rationale for their use in strategies designed to prevent post-angioplasty restenosis is based on the ostensible ability of these agents to selectively injure dividing SMC while leaving non-proliferating cells undamaged (Lovqvist et al., 1993).

Vincristine, actinomycin D, and methotrexate. While successful in preventing SMC proliferation after endothelial injury in animals (Barath et al., 1989), the potential clinical toxicity of these drugs prohibits their realistic application in the human model.

Antiproliferative Agents

The antiproliferative agents studied have included colchicine, glucocorticoids, cilazapril, angiopeptin, and trapidil. The theoretical basis for their use in strategies designed to prevent post-angioplasty restenosis is derived from the principal role that SMC proliferation plays in the process of late restenosis.

Colchicine. Colchicine interferes with proper microtubule function by binding tubulin, the subunit protein of microtubules. Consequently, it is a potent inhibitor of cell division. While successful at preventing restenosis after balloon injury in various animal models (Bilazarian et al., 1989), a recent randomized, placebo-controlled trial has shown that colchicine is ineffective at preventing restenosis in humans (O'Keefe et al., 1992).

Corticosteroids. Steroids have well-characterized antiinflammatory and antiproliferative properties. While hydrocortisone has demonstrated a synergistic inhibition of SMC proliferation when combined with low molecular weight heparin (Gordon et al., 1987), a multicenter controlled trial has revealed that corticosteroids yield no beneficial effect on restenosis (Pepine et al., 1990).

Cilazapril. In addition to being a vasoconstrictor, angiotensin II is able to stimulate SMC proliferation and matrix formation (Lange et al., 1993). Cilazapril, an angiotensin

converting enzyme (ACE) inhibitor, has been shown to reduce restenosis in experimental angioplasty (Bilazarian et al., 1991). However, two large multicenter trials evaluating the long-term effects of cilazapril on restenosis have shown no difference between treated and control patients (MERCATOR, 1992; Faxon et al., 1992).

Somatostatin and angiopeptin. Somatostatin is a known potent inhibitor of growth hormone secretion. Angiopeptin, a somatostatin analogue, has been shown to inhibit myointimal proliferation in animal models following endothelial injury (Lundergan et al., 1991). Multicenter trials in both Europe and the United States, however, have failed to demonstrate any beneficial impact of angiopeptin on post-angioplasty restenosis (Faxon and Currier, 1995).

Trapidil. Trapidil (triazolopyrimidine) possesses antiproliferative effects by virtue of its ability to antagonize PDGF. Its success in preventing post-angioplasty restenosis in atherosclerotic rabbits (Liu et al., 1990) has prompted clinical trials. While two small studies have shown trapidil to be effective at preventing restenosis (Okamoto et al., 1992; STARC, 1993), further investigation is warranted.

4. Photochemotherapy with 8-MOP and visible light

Photochemotherapy

Photochemotherapy is a therapeutic modality that makes use of drugs which can be pharmacologically activated by light. Upon irradiation, these drugs which possess low intrinsic activity are transformed into highly reactive compounds. Photochemotherapy has been used safely and effectively in the treatment of a variety of hyperproliferative skin disorders for centuries. More recently, studies have been performed to assess the potential efficacy of a variety of photochemotherapeutic agents in the control of SMC proliferation.

Chloroaluminum-sulfonated phthalocyanine. Chloroaluminum-sulfonated phthalocyanine, a photosensitizer currently under evaluation for the treatment of malignant lesions, has been shown to effectively reduce intimal hyperplasia in a rat model (Ortu et al., 1992). While this treatment regimen demonstrates promise for potential application in the prevention of post-angioplasty restenosis, its effectiveness in the human model has yet to be investigated.

Hematoporphyrin compounds. Both *in vivo* and *in vitro* studies on the effects of hematoporphyrin compounds on SMC proliferation have also suggested their potential use in therapies designed to inhibit neointima formation (Litvack et al., 1985; Dartsch et al., 1990). These compounds, however, are associated with a cutaneous phototoxicity for

up to several weeks after administration. This has, in general, limited their clinical application to experimental treatments involving certain malignant cancers (March et al., 1993).

Photofrin. Photofrin is yet another photosensitizer which has been shown to successfully reduce intimal hyperplasia in animals. Photoactivated with 630 nm light, Photofrin was shown to decrease intimal thickening in a rabbit model by approximately 50% (Eton et al., 1992). The toxicity of Photofrin in humans, however, has yet to be resolved.

Moreover, a recent study demonstrating that photoactivated Photofrin can induce microtubule depolymerization in human EC (Sporn and Foster, 1992) calls its suitability for human application into question. As damaged EC contribute to the process of restenosis by stimulating SMC proliferation (see “Phase II of Vascular Wound Healing: Granulation,” Chapter 2), a more ideal treatment regimen might entail the use of a drug which could selectively inhibit SMC proliferation without causing damage to EC.

8-Methoxypsoralen (8-MOP)

Photochemotherapy with 8-methoxypsoralen (8-MOP) dates as far back as the 15th century B.C. Ancient manuscripts document the use of this compound, extracted from psoralen-containing plants, in the treatment of vitiligo. Photoactivation during this time was achieved via exposure to natural sunlight (Roelandts, 1991).

Today, photochemotherapy with 8-MOP has been approved by the Food and Drug Administration (FDA) for the treatment of a variety of skin diseases. Treatment typically

consists of oral or intravenous administration of 8-MOP followed by photoactivation with high-intensity UVA bulbs in affected areas of skin.

Given its excretion rate of approximately 90% within the first 12 hours of administration (Gupta and Anderson, 1987), 8-MOP exhibits minimal long-term phototoxicity. Its established long-term safety and therapeutic efficacy have helped it to become the foremost photosensitizer employed in all of photomedicine (Gasparro, 1990). While photochemotherapy with 8-MOP is most commonly used in the treatments of psoriasis and vitiligo, its clinical application has spanned more than 40 other diseases (Roelandts, 1991).

Clinical applications of photochemotherapy with 8-MOP

| | |
|---|-----------------------------|
| acne vulgaris | ichthyosis |
| alopecia areata | impetigo herpetiformis |
| atopic dermatitis | lichen planus |
| basal-cell and squamous cell carcinoma | lymphomatoid papulosis |
| chronic actinic dermatitis | mycosis fungoides |
| chronic hyperkeratotic dermatitis | nodular prurigo |
| chronic urticaria | palmoplantar pustulosis |
| contact dermatitis | papuloerythroderma |
| Darier's disease (keratosis follicularis) | parapsoriasis |
| disseminated superficial actinic porokeratosis | pityriasis alba |
| dyshidrotic eczema | pityriasis lichenoides |
| epidermodysplasia verruciformis | pityriasis rubra pilaris |
| erythema elevatum et diutinum | polymorphous light eruption |
| erythrodermia congenitalis progressiva symmetrica | psoriasis |
| erythropoietic protoporphyria | purpura |
| follicular mucinosis | scleromyxedema |
| graft-versus-host-reaction | seborrheic dermatitis |
| granuloma annulare | solar urticaria |
| granuloma faciale | acantholytic dermatosis |
| Hailey-Hailey disease | urticaria pigmentosa |
| herpes | vitiligo |
| hydroa vacciniforme | warts |
| hyperkeratosis lenticularis persistans | |

Table 4-1. Summary of some of the indications for which photochemotherapy with 8-methoxypsoralen has been applied. Table modified from Roelandts, 1991.

8-MOP is a planar tricyclic furocoumarin. Its 5-member furan ring and 6-member pyrone ring are connected linearly by a benzene ring.

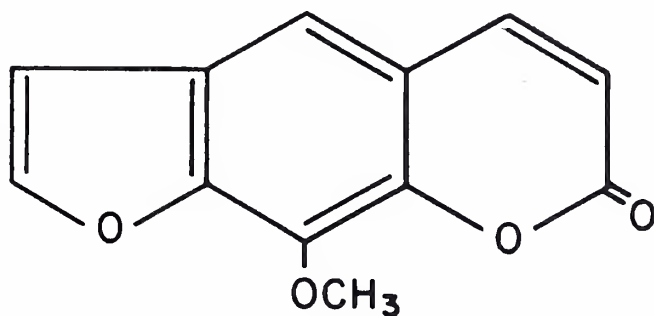


Figure 4-1. Diagram of 8-methoxypsoralen. Figure taken from Gasparro, 1994.

When exposed to cells in darkness, 8-MOP molecules can easily diffuse into the nuclei and intercalate between DNA base pairs. While inert in the dark, 8-MOP forms photoadducts with DNA when exposed to light. These photoadducts represent the key to 8-MOP's effectiveness in anti-proliferative photochemotherapies, as they presumably cause an arrest in DNA synthesis (Roelandts, 1991) and hence cell replication.

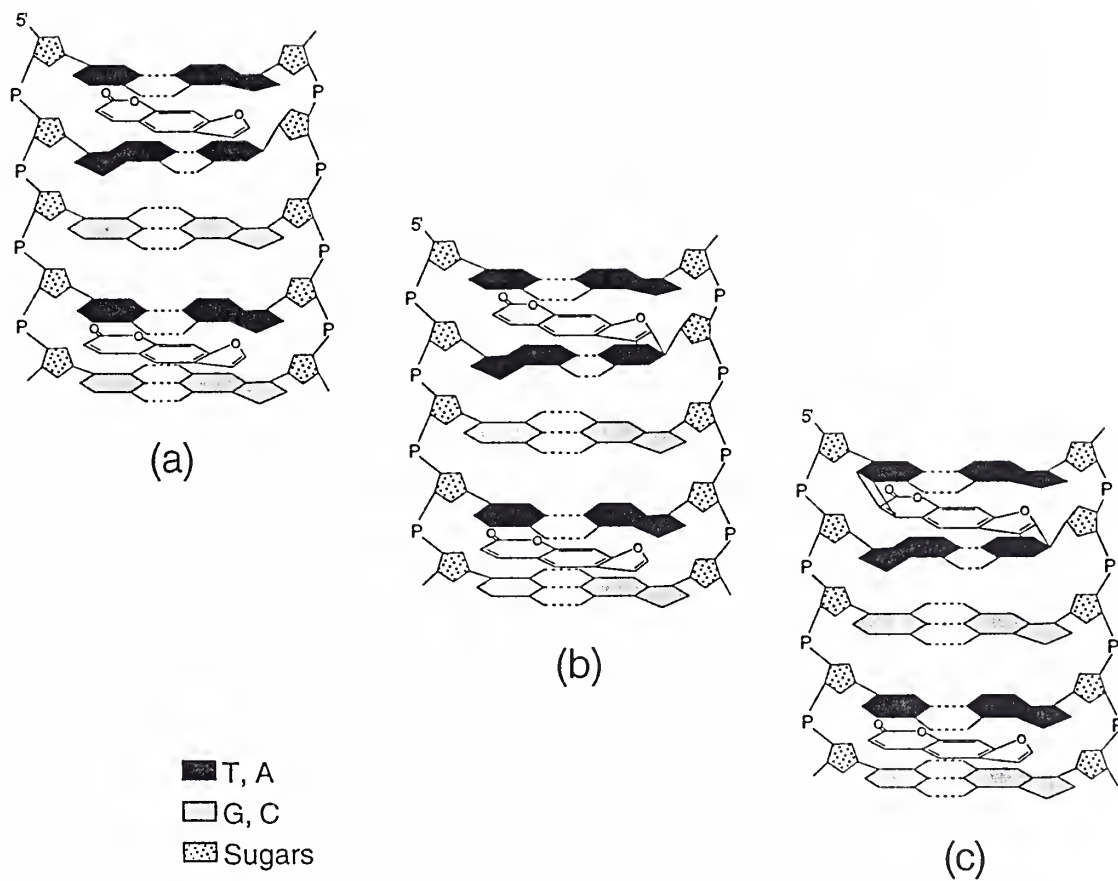


Figure 4-2. Schematic demonstrating photoadduct formation by 8-MOP. a: Two 8-MOP molecules intercalated between DNA base pairs. As 8-MOP forms photoadducts primarily with thymine, the upper molecule is positioned to form a crosslink, while the lower molecule is positioned to form a 3, 4-monoadduct. b: the upper molecule forms a 4', 5'-monoadduct with the DNA. c: additional formation of a 3, 4-monoadduct converts the former 4', 5'-monoadduct into a crosslink. Not all 8-MOP molecules form photoadducts with the DNA, as seen in the lower molecule. Figures taken from Gasparro, 1994.

Three distinct types of photoadduct form between 8-MOP and DNA upon light-activation. These include two types of monoadduct (a 4', 5'-monoadduct and 3, 4-monoadduct) and a crosslink.

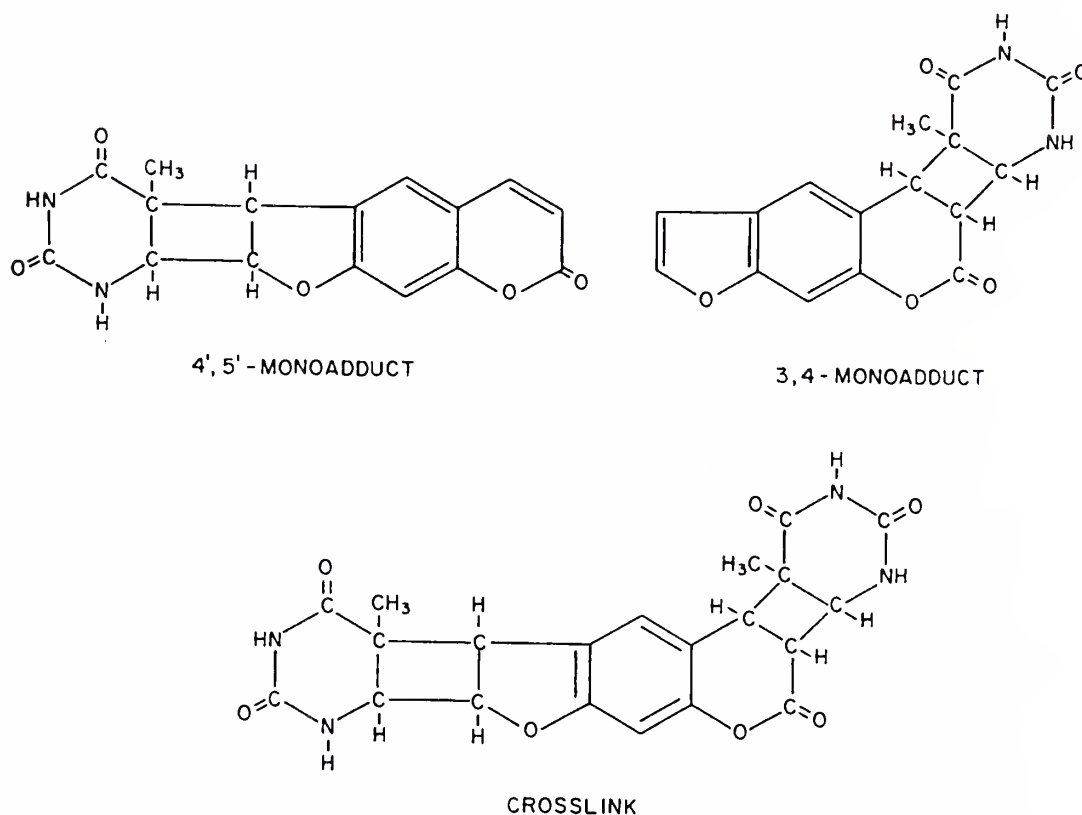


Figure 4-3. Diagrams of the 4', 5'-monoadduct; 3, 4-monoadduct; and crosslink. Figure taken from Gasparro, 1994.

All three photoadducts are the product of 2+2 photocycloadditions to pyrimidine bases, primarily thymine (Gasparro et al., 1990).

The absorption spectrum of 8-MOP has been measured over the range of 200-500 nm with a peak absorbance found at the 200-300 nm wavelengths (Gasparro et al., 1993).

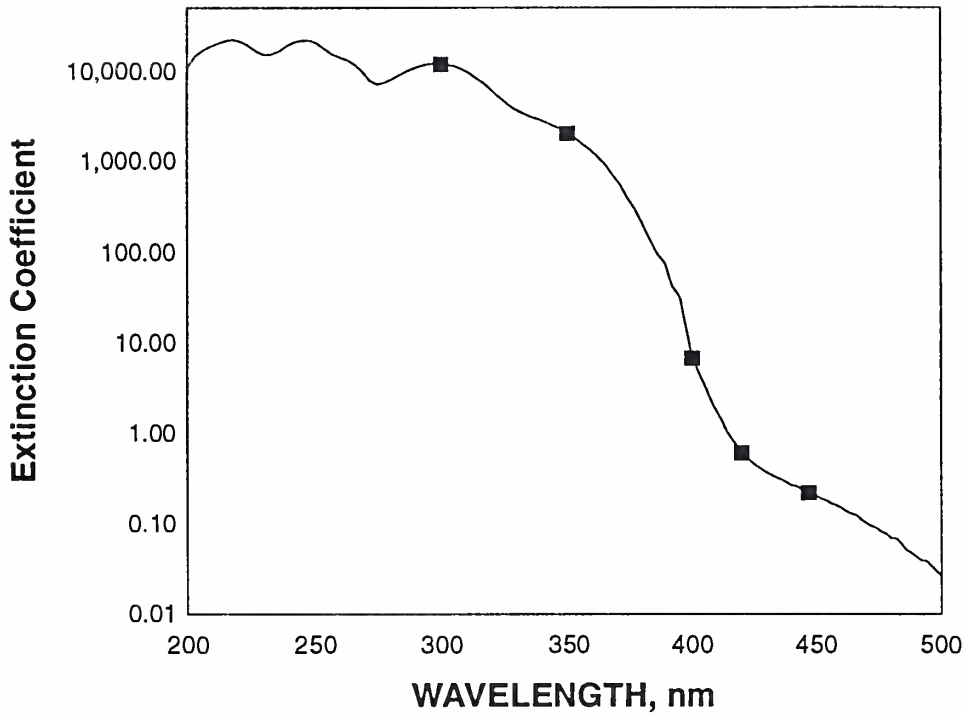


Figure 4-4. Absorption spectrum for 8-MOP. Note the extinction coefficients corresponding to the wavelengths with the filled squares are: 300 nm, 11800 $\text{cm}^{-1} \text{M}^{-1}$; 355 nm, 2016 $\text{cm}^{-1} \text{M}^{-1}$; 400 nm, 6.8 $\text{cm}^{-1} \text{M}^{-1}$; 419 nm, 0.60 $\text{cm}^{-1} \text{M}^{-1}$; and 447 nm, 0.22 $\text{cm}^{-1} \text{M}^{-1}$. Figure taken from Gasparro, 1994.

While 8-MOP has traditionally been activated with long-wavelength ultraviolet radiation, recent studies have shown that photoactivation with visible light results in a significant reduction in crosslink formation. The percentage of crosslinks formed by 8-MOP photoactivated at 419 nm is less than one fourth that formed when activated with ultraviolet radiation (UVA, 320-400 nm), while the percentage of crosslinks formed by 8-

MOP photoactivated at 447 nm is almost one fiftieth that formed when activated with UVA.

Adduct Formation and Distribution in SMC

| Wavelength (dose) nm (J/cm ²) | [8-MOP] μg/mL | Total Adducts per mbp | 4',5'-MA | 3,4-MA | XL |
|--|------------------|--------------------------|----------|--------|-----|
| UVA (2) | 1.0 | 88.0 | 41% | 12% | 47% |
| 419 nm (7) | 1.0 | 9.0 | 84% | 13% | 3% |
| 419 nm (12) | 1.0 | 13.5 | 78% | 12% | 11% |
| 447 nm (12) | 20.0 | 22.4 | 90% | 9% | 1% |

Table 4-1. Adduct formation and distribution in SMC. MA = monoadducts; XL = crosslinks. Table modified from Sumpio et al., 1994.

It has been postulated that this reduction in crosslink formation may serve to reduce the drug's mutagenicity and hence enhance its therapeutic efficacy (Gasparro et al., 1993; Sumpio et al., 1994).

5. Statement of Purpose

The purpose of the present study was to address the problem of post-angioplasty restenosis by evaluating the effects of 8-MOP photoactivated with 447 nm visible light on vascular cells (SMC and EC) *in vitro*.

The photosensitizer 8-MOP was chosen for its established long-term safety. As described in the previous chapter, this FDA-approved drug is commonly used and well-tolerated in therapies for a variety of dermatologic diseases. Its administration is associated with minimal long-term phototoxicity secondary to a rapid clearance rate.

Photoactivation with visible light rather than ultraviolet light was favored for the significant reduction in crosslink formation associated with visible-light photoactivation (Gasparro et al., 1993; Sumpio et al., 1994). Additionally, visible light was chosen as it offers both a deeper tissue penetration and superior compatibility with fiber-optic applications than ultraviolet light.

The 447 nm wavelength used in the experiments was chosen primarily for the immediate availability of the 447 nm laser. This laser is presently available on the market, as it is being manufactured for application in other clinical scenarios.

It is hypothesized that photochemotherapy with 8-MOP and visible light can result in the selective inhibition of SMC proliferation and may thus represent a novel approach to the prevention of post-angioplasty restenosis.

6. Experimental Methods^a

Cell Culture

Bovine SMC and EC were obtained from calf thoracic aortas by means of a previously described explant method (Sumpio and Banes, 1988). Thoracic aortas were removed aseptically from calves and transferred on ice to a tissue culture facility. Under a laminar flow hood, the peri-aortic fat was carefully trimmed and discarded. A longitudinal incision was then made along the length of the aorta and the lumen exposed. After being rinsed five to six times with Phosphate Buffered Saline (PBS), the EC were carefully removed with a blade and placed in a culture dish containing growth media consisting of Dulbecco's Modified Eagle's Medium F-12 (DMEM F-12) supplemented with antibiotics (300 U/mL penicillin, 300 U/mL streptomycin), deoxycytidine/deoxythymidine, and 10% (v/v) heat-inactivated fetal bovine serum. Following removal of the EC, the exposed medial layer of aorta was rinsed thoroughly with PBS and 2 mm² biopsies obtained and placed in a culture dish containing growth media consisting of Dulbecco's Modified Eagle's Medium (DMEM) supplemented with antibiotics (300 U/mL penicillin, 300 U/mL streptomycin), 0.2 M L-glutamine, and 10% (v/v) heat-inactivated fetal bovine serum.

^a All procedures described in this methods chapter, barring those described in the Size and Photoadduct Formation section, were performed by the author.

Both cell types were then incubated at 37° C and 5% CO₂ until explants could be detected. The presence of EC or SMC was confirmed by direct visualization via light microscopy. SMC were identified by their typical hill-and-valley formation at confluency and hence could be distinguished from fibroblasts, which exhibit a whorl-like appearance.

Both cell types were subcultured with 0.01% trypsin/ethylene diamino tetraacetic acid (EDTA) and cultured on 75 cm² tissue culture flasks, maintained in their respective growth media as described above, and grown at 37° C and 5% CO₂. Cells used in the experiments were obtained from subsequent passages subcultured with 0.01% trypsin/EDTA. All experiments were performed using cells of passage seven or less.

Chemicals

A 1 mg/mL stock solution of 8-MOP (Sigma Chemical Co., St. Louis, MO) was prepared in absolute ethanol. The different concentrations of 8-MOP used in the experiments were obtained by appropriate dilution of this stock and subsequently verified by spectroscopy or high-performance liquid chromatography (HPLC) analysis.

Experimental Protocol

Bovine aortic SMC or EC were detached and collected from the tissue culture flasks by trypsinization with 0.01% trypsin/EDTA. They were then seeded in polystyrene 12-well plates at a density of 5,000 to 10,000/cm² and placed in an incubator at 37° C and 5% CO₂. Following a 24-hour attachment period, the cells were rinsed once with Phosphate Buffered Saline (PBS) and then incubated with 1, 20, or 50 µg/mL 8-MOP for 30 minutes

in the dark. The plates containing control cells were wrapped with aluminum foil prior to incubation so as to prevent ambient light exposure.

All plates, including the control plates still wrapped in foil, were then exposed to 12.0 J/cm² visible light (447 nm) in a photochemical reactor (Southern New England Ultraviolet Co., Branford, CT) equipped with lamps spaced evenly over an arc at 22.5° intervals. The light doses being administered were determined using a calibrated silicon diode UV250BQ (EG&G, Montgomeryville, PA). Following irradiation, the 8-MOP media was aspirated and replaced with fresh growth media, and the plates were returned to the incubator. Growth media was aspirated and replaced with fresh media every 48 hours.

Cell Counts

Cell counts were performed on days 0, 1, 3, 5, 7, 10, and 14 following the initiation of each experiment. Growth media from each cell well was collected and later analyzed for the presence of LDH to ascertain cell death. Meanwhile, SMC or EC from each cell well were rinsed once with PBS, detached by treatment with 1% trypsin/EDTA, and collected in aliquots. The number of cells in each aliquot was then determined using a Coulter Counter (Model ZM, Hialeah, FL).

Cell Migration

SMC or EC were collected and seeded in Nunc 2-well chamber slides at near confluent densities (approximately 70,000/cm²). They were then incubated for an attachment period

of 48 hours. A second set of cells was incubated for an additional 2 hours in 10 $\mu\text{g}/\text{mL}$ mitomycin C. The purpose of the mitomycin was to inhibit the potentially confounding effect of cell proliferation on cell migration.

All cells were then rinsed with PBS, treated with 8-MOP, and exposed to light in the same manner as described previously. Cells treated with 0 $\mu\text{g}/\text{mL}$ 8-MOP and exposed to visible light served as the control cells for these experiments. Before the 8-MOP media was aspirated and replaced with fresh growth media, a sterile wound was created across the middle of the well using a sterile blade, and the cells on one side of the wound were completely removed. On the specified days, the appropriate cells were rinsed with PBS, fixed with 10% formalin, and stored in PBS. At a later time, they were stained with 2.5% (v/v) crystal violet for 1 minute, rinsed twice with PBS, and then examined and photographed under a light microscope.

Cell Morphology

SMC were collected and seeded in Nunc 2-well chamber slides at a density of approximately 10,000 to 20,000/cm². They were then incubated for an attachment period of 24 hours. Afterwards, the cells were rinsed with PBS, treated with 8-MOP, exposed to light, incubated, and maintained in the same manner as described in the Experimental Protocol section. On the specified days, the appropriate cells were rinsed with PBS, fixed with 10% formalin, and stored in PBS. At a later time, they were stained with 2.5% (v/v) crystal violet for 1 minute, rinsed twice with PBS, and then examined and photographed under a light microscope.

Cell Size^b

SMC and EC were collected and seeded in polystyrene 12-well plates at a density of 5,000 to 10,000/cm² and allowed to attach over a 24 hour period. Treated cells were incubated with 20 µg/mL 8-MOP for 30 minutes in the dark and then exposed to 12.0 J/cm² 447 nm visible light. As in other experiments, cells treated with 8-MOP but not exposed to light served as control cells. Cells neither treated with 8-MOP nor exposed to light and cells not treated with 8-MOP but exposed to light served as additional controls for this set of experiments.

Cell size was measured with a Coulter Counter equipped with a Channelyzer (Coulter, Hialeah, FL) on days 3, 5, 7, 10, and 14 following the initiation of each experiment.

SMC or EC from the cell wells were rinsed once with PBS, detached by treatment with 1% trypsin/EDTA, and then collected in 500 µL aliquots. The sizes of 10⁴ cells per aliquot were measured and recorded.

Photoadduct Formation^b

SMC and EC were collected and seeded in polystyrene 12-well plates at a density of 5,000 to 10,000/cm². The cells were then incubated with 20 µg/mL of 8-MOP including trace amounts of [³H]8-MOP (specific activity = 83 Ci/mmol; Amersham International, Arlington Heights, IL) for 30 minutes in the dark and irradiated with 32.0 J/cm² 447 nm visible light. Afterwards, the cells were trypsinized and suspended in 500 µL of 50

^b Studies performed with the help of Xiu-Jie Wang and Francis Gasparro.

mmol/L TRIS/150 mmol/L NaCl/100 mmol/L EDTA (pH 8), and the DNA was isolated as described previously (Bevilacqua et al., 1991; Olack et al., 1993). DNA concentration was determined by UV spectroscopy (LKB Ultrospec II), and the molar concentration in terms of nucleotide units (base pairs) was computed from the absorbance at 260 and 280 nm.

The DNA was hydrolyzed enzymatically with 1 Unit/mL P₁ nuclease and 0.1 Unit/mL DNase I in water and then applied to an ODS reversed phase column (Regis Rexchrome, 4.6x250 mm; 5 micron, Morton Grove IL) for analysis. The [³H] 8-MOP photoadducts (4',5' monoadducts; 3,4 monoadducts; and cross-links) were detected by scintillation analysis of HPLC fractions collected during the analysis of enzymatically hydrolyzed DNA isolated from cells.

Statistical Analysis

Statistical analyses (ANOVA and Student's t Test) were performed using Systat for Windows (Evanston, IL) and Sigmaplot (Jandel, San Rafael, CA).

7. Results

SMC Proliferation

The effects of 12.0 J/cm^2 447 nm visible light-activated 8-MOP on SMC proliferation are shown in the following representative growth curves (Figures 7-1, 7-2, and 7-3). The lowest dose of 8-MOP ($1 \text{ }\mu\text{g/mL}$) had no effect on SMC proliferation (Figure 7-1). The intermediate dose of 8-MOP ($20 \text{ }\mu\text{g/mL}$) yielded transient and reversible inhibition of SMC proliferation, as evidenced by the recovery in the growth curve (Figure 7-2). The highest dose of 8-MOP ($50 \text{ }\mu\text{g/mL}$) was cytotoxic to the SMC (Figure 7-3). The growth of SMC treated with drug or light alone at each dose was not significantly different from control, untreated SMC (data not shown). The results of triplicate experiments per drug dose were combined and expressed as percent recovery for days 3, 5, 7, and 10 (Figure 7-4), where percent recovery represents the number of cells per aliquot divided by the number of cells in the corresponding control aliquot. Differences in percent recovery between cells treated with $1 \text{ }\mu\text{g/mL}$ and the two higher doses were statistically significant ($p < 0.05$).

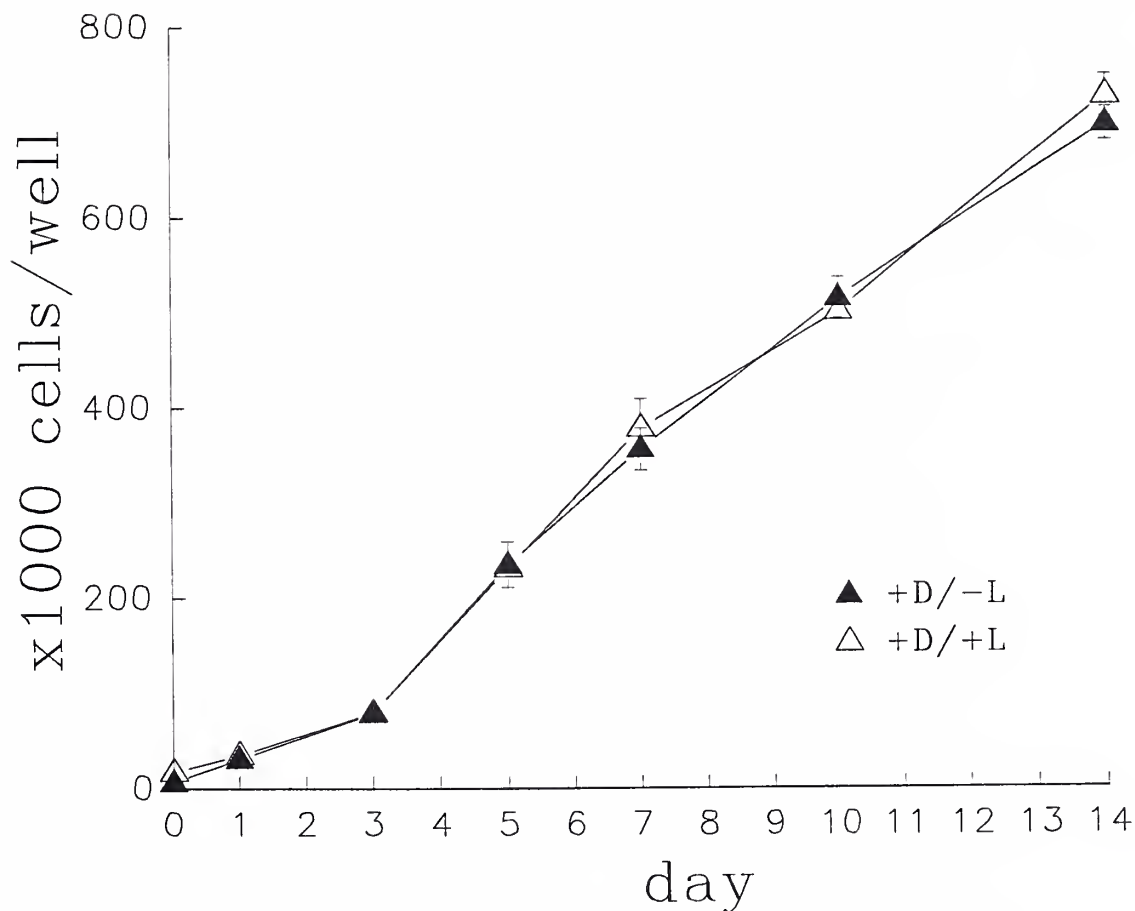
SMC; 1 $\mu\text{g}/\text{mL}$ 8-MOP

Figure 7-1. Proliferation curves for SMC treated at 1 $\mu\text{g}/\text{mL}$ 8-MOP both with and without light. D = drug; L = light; hence, control cells are represented by dark triangles and treated cells by clear triangles. No difference is seen between control and treated cells.

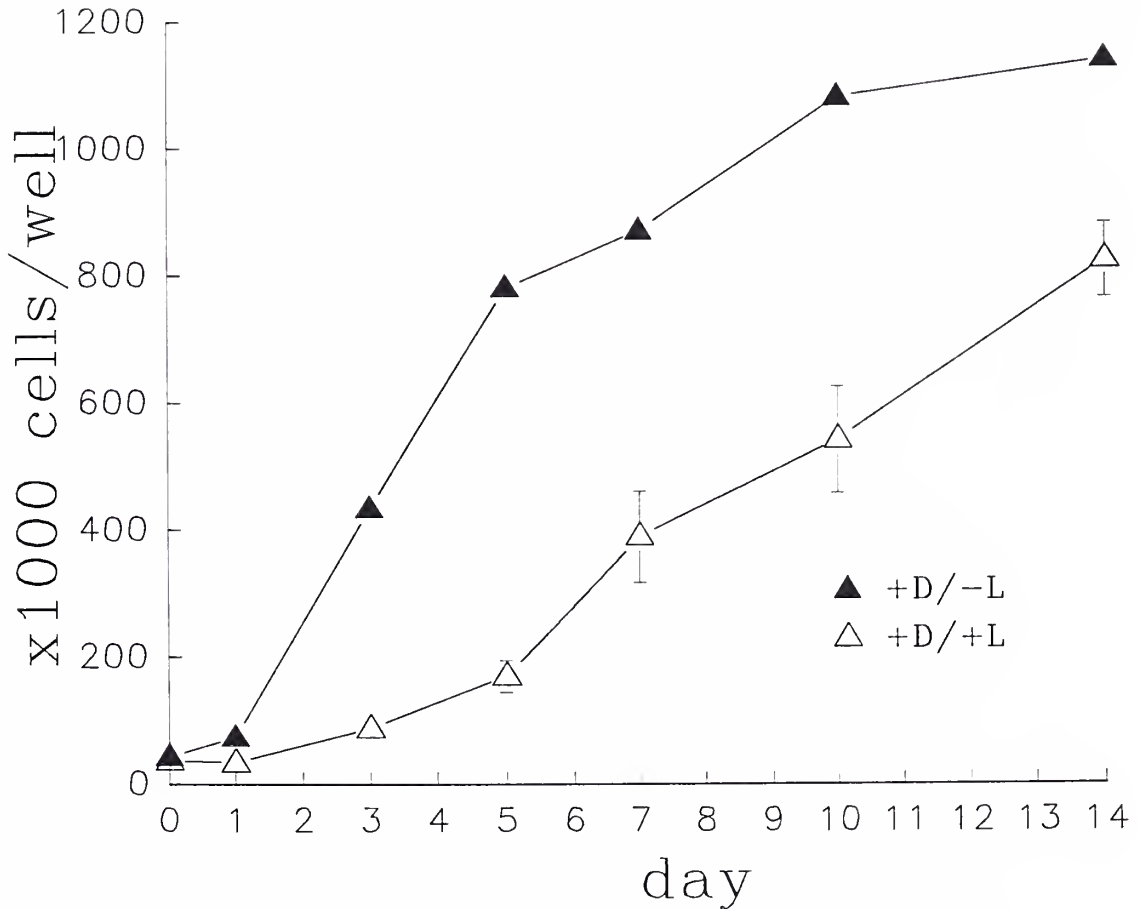
SMC; 20 $\mu\text{g}/\text{mL}$ 8-MOP

Figure 7-2. Proliferation curves for SMC treated at 20 $\mu\text{g}/\text{mL}$ 8-MOP both with and without light. D = drug; L = light; hence, control cells are represented by dark triangles and treated cells by clear triangles. Transient and reversible inhibition of SMC proliferation is evidenced by the recovery in the growth curve for treated cells.

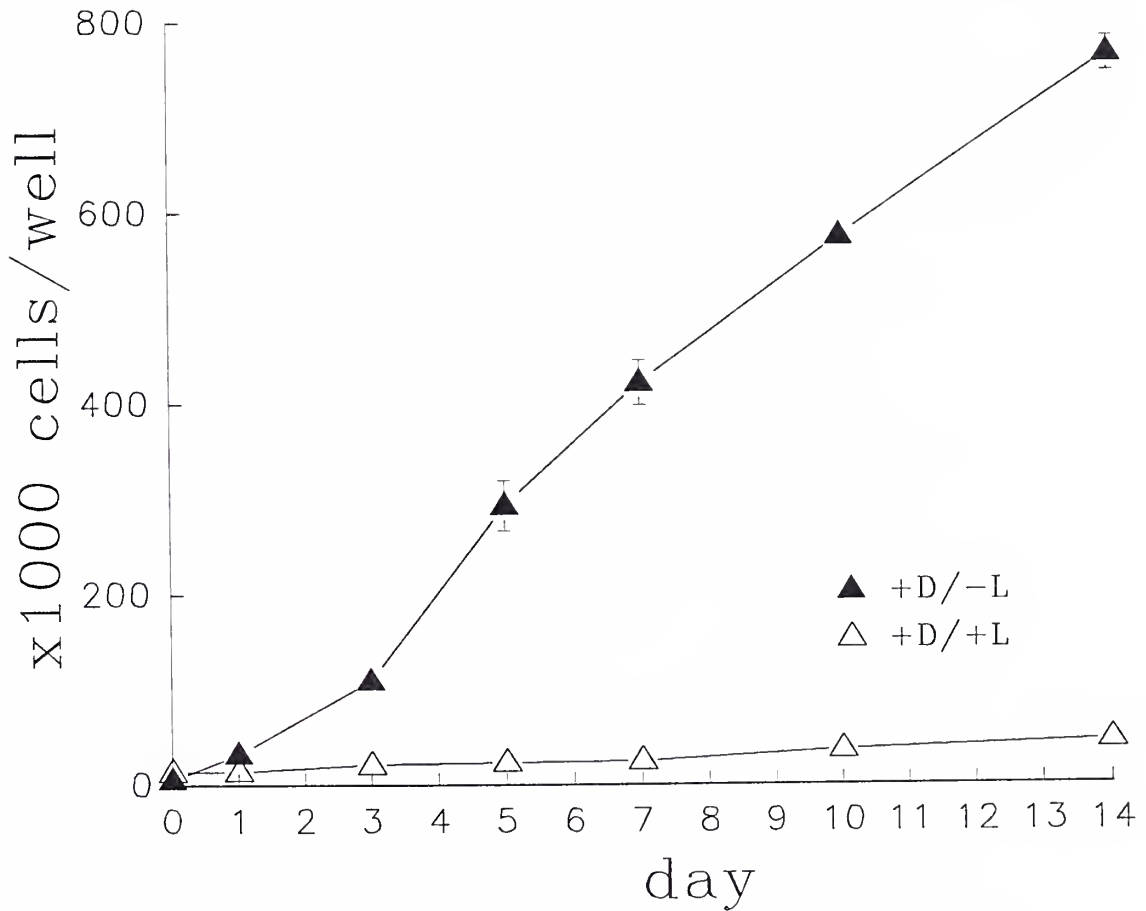
SMC; 50 $\mu\text{g}/\text{mL}$ 8-MOP

Figure 7-3. Proliferation curves for SMC treated at 50 $\mu\text{g}/\text{mL}$ 8-MOP both with and without light. D = drug; L = light; hence, control cells are represented by dark triangles and treated cells by clear triangles. Treatment at this dose of 8-MOP appears to be cytotoxic to the SMC as no recovery is seen in the growth curve for treated cells.

Effects of 8-MOP on SMC at 1, 20, and 50 $\mu\text{g}/\text{mL}$ 8-MOP

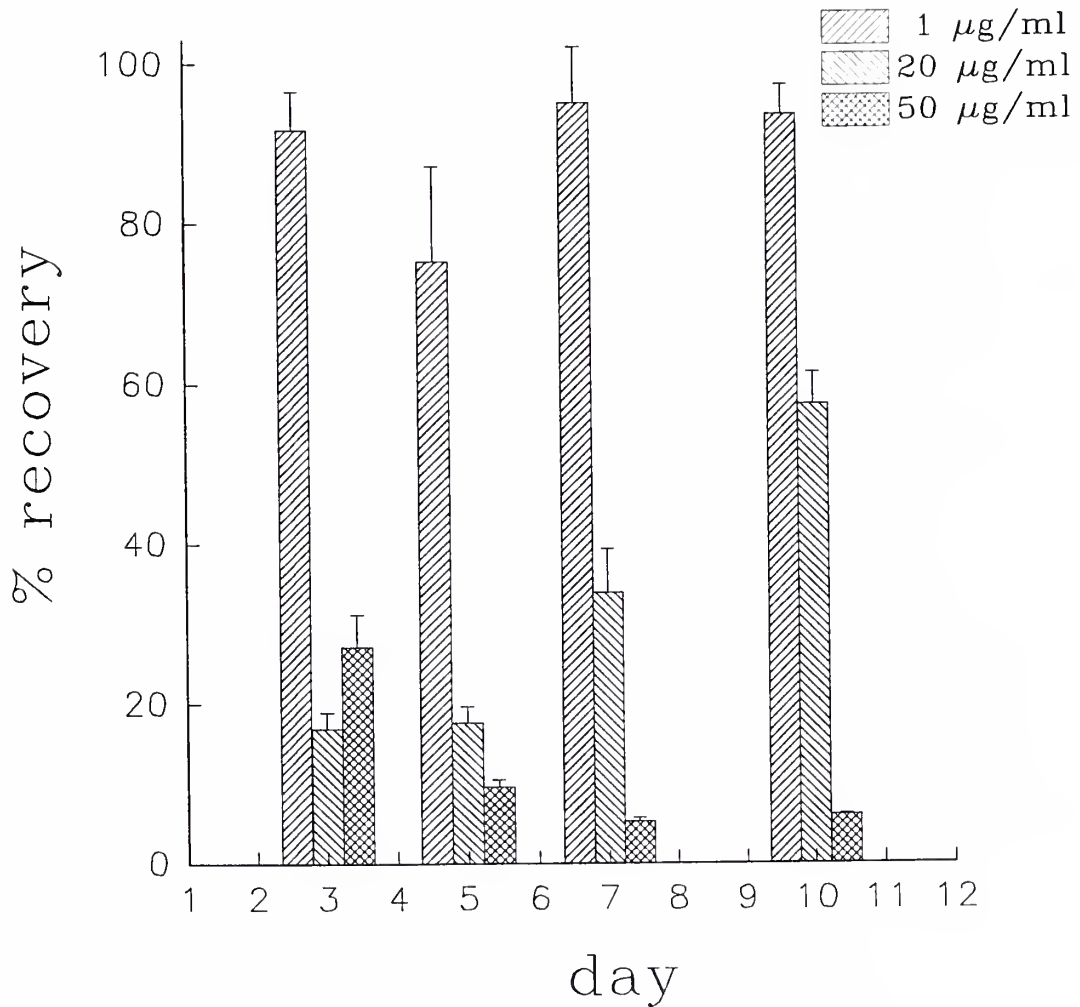


Figure 7-4. Summary graph of triplicate experiments performed on SMC at 1, 20, and 50 $\mu\text{g}/\text{mL}$ 8-MOP. Percent recovery = number of treated cells/number of control cells. No effect is apparent at 1 $\mu\text{g}/\text{mL}$ 8-MOP. Inhibition with gradual recovery of SMC proliferation is seen at 20 $\mu\text{g}/\text{mL}$ 8-MOP. Cell death is seen at 50 $\mu\text{g}/\text{mL}$ 8-MOP.

EC Proliferation

The effects of 12.0 J/cm^2 447 nm visible light-activated 8-MOP on EC proliferation are shown in the following representative growth curves (Figures 7-5, 7-6, and 7-7). As seen in the SMC experiments, the lowest dose of 8-MOP ($1 \text{ }\mu\text{g/mL}$) had no effect on EC proliferation (Figure 7-5). Likewise, the growth of EC treated with drug or light alone at each dose was not significantly different from control, untreated EC (data not shown). At both the intermediate and highest doses of 8-MOP (20 and $50 \text{ }\mu\text{g/mL}$, respectively), however, inhibition of EC proliferation was transient and reversible, as evidenced by the recovery in the growth curves (Figures 7-6 and 7-7). The results of triplicate experiments per drug dose were combined and expressed as percent recovery for days 3, 5, 7, and 10 (Figure 7-8), where percent recovery represents the number of cells per aliquot divided by the number of cells in the corresponding control aliquot. Differences in percent recovery between cells treated with $1 \text{ }\mu\text{g/mL}$ and the two higher doses were statistically significant ($p < 0.05$) only for day 5.

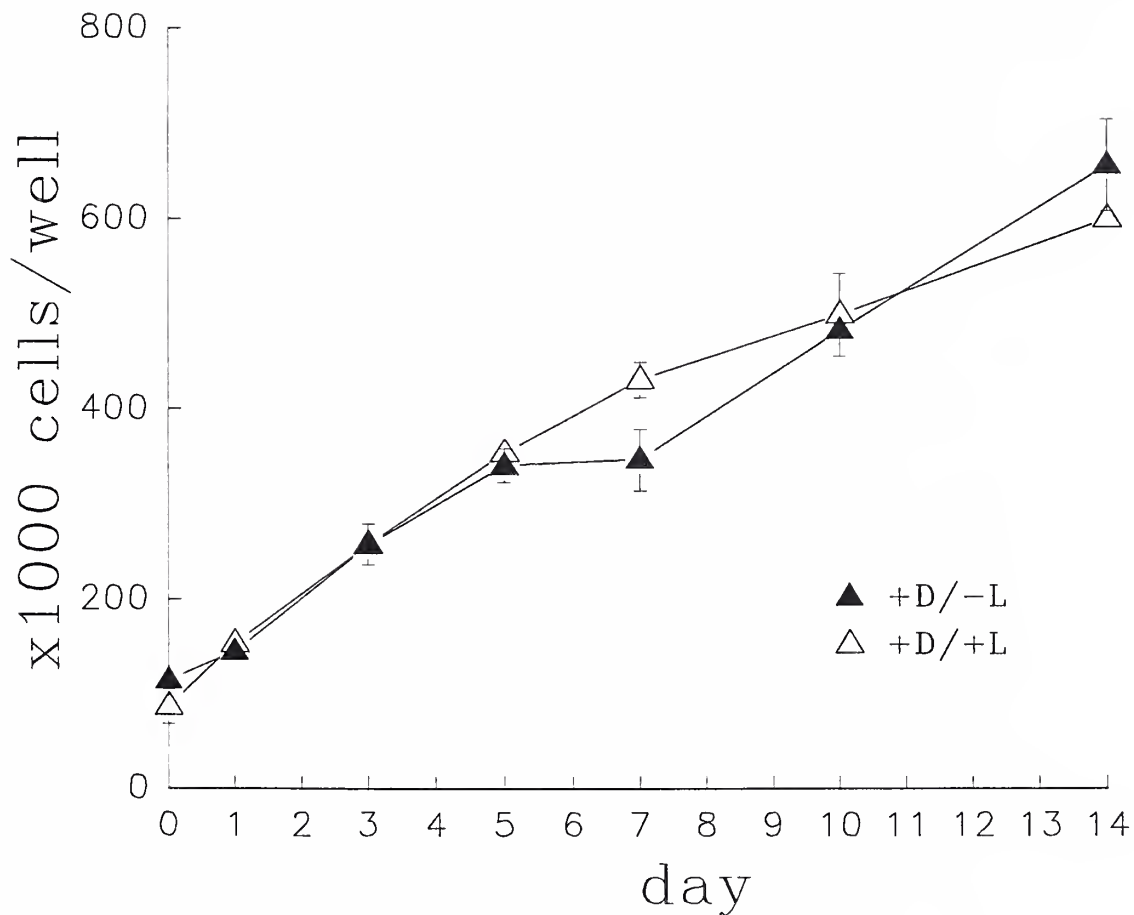
EC; 1 $\mu\text{g}/\text{mL}$ 8-MOP

Figure 7-5. Proliferation curves for EC treated at 1 $\mu\text{g}/\text{mL}$ 8-MOP both with and without light. D = drug; L = light; hence, control cells are represented by dark triangles and treated cells by clear triangles. No difference is seen between control and treated cells.

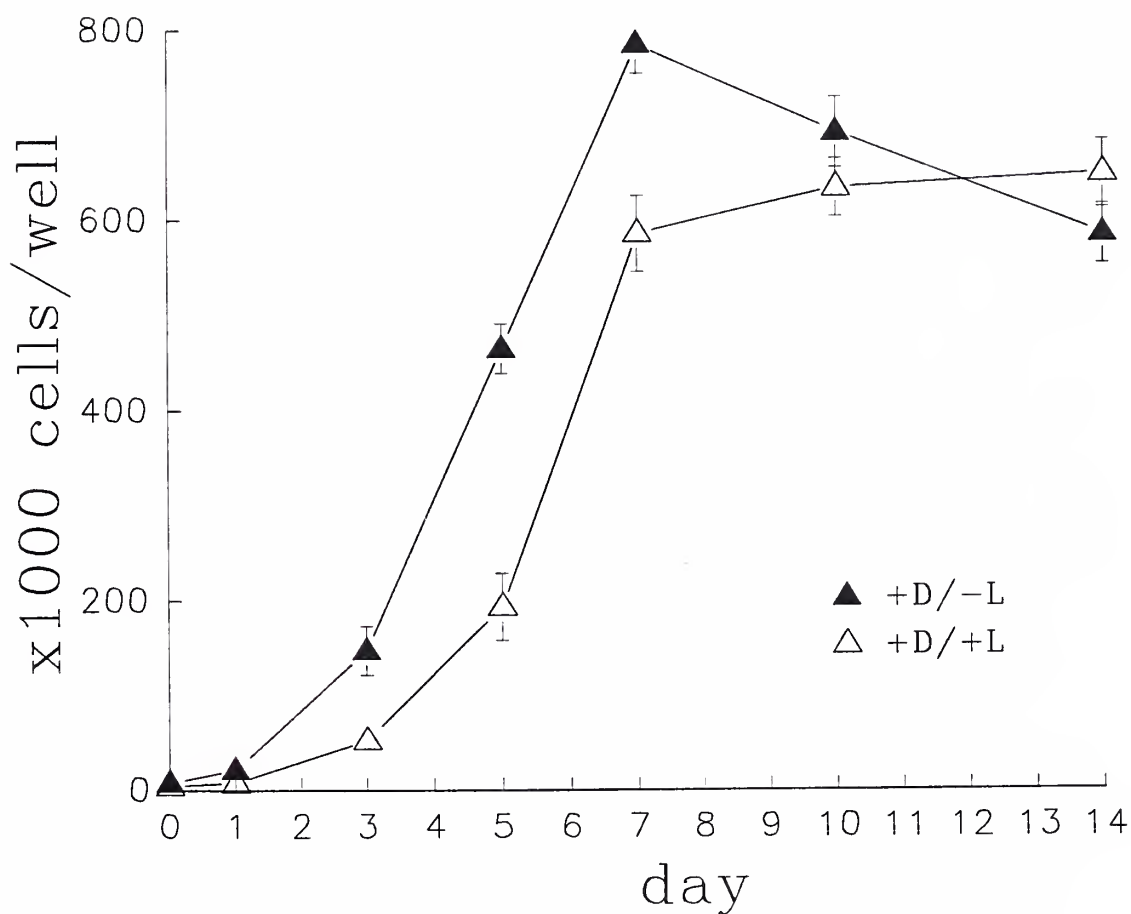
EC; 20 $\mu\text{g}/\text{mL}$ 8-MOP

Figure 7-6. Proliferation curves for EC treated at 20 $\mu\text{g}/\text{mL}$ 8-MOP both with and without light. D = drug; L = light; hence, control cells are represented by dark triangles and treated cells by clear triangles. Transient and rapidly reversible inhibition of EC proliferation is evidenced by the recovery in the growth curve for treated cells.

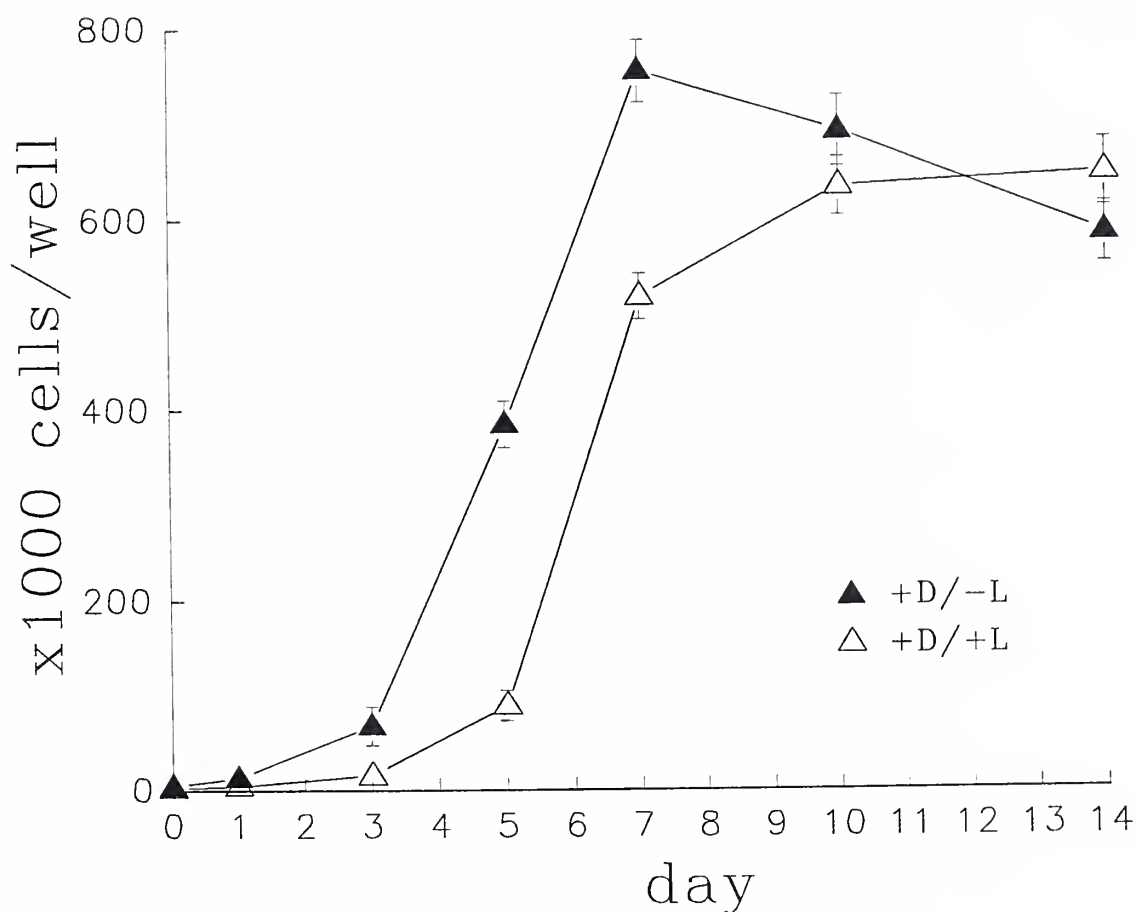
EC; 50 $\mu\text{g}/\text{mL}$ 8-MOP

Figure 7-7. Proliferation curves for EC treated at 50 $\mu\text{g}/\text{mL}$ 8-MOP both with and without light. D = drug; L = light; hence, control cells are represented by dark triangles and treated cells by clear triangles. Transient and rapidly reversible inhibition of EC proliferation is evidenced by the recovery in the growth curve for treated cells.

Effects of 8-MOP on EC at 1, 20, and 50 $\mu\text{g}/\text{mL}$ 8-MOP

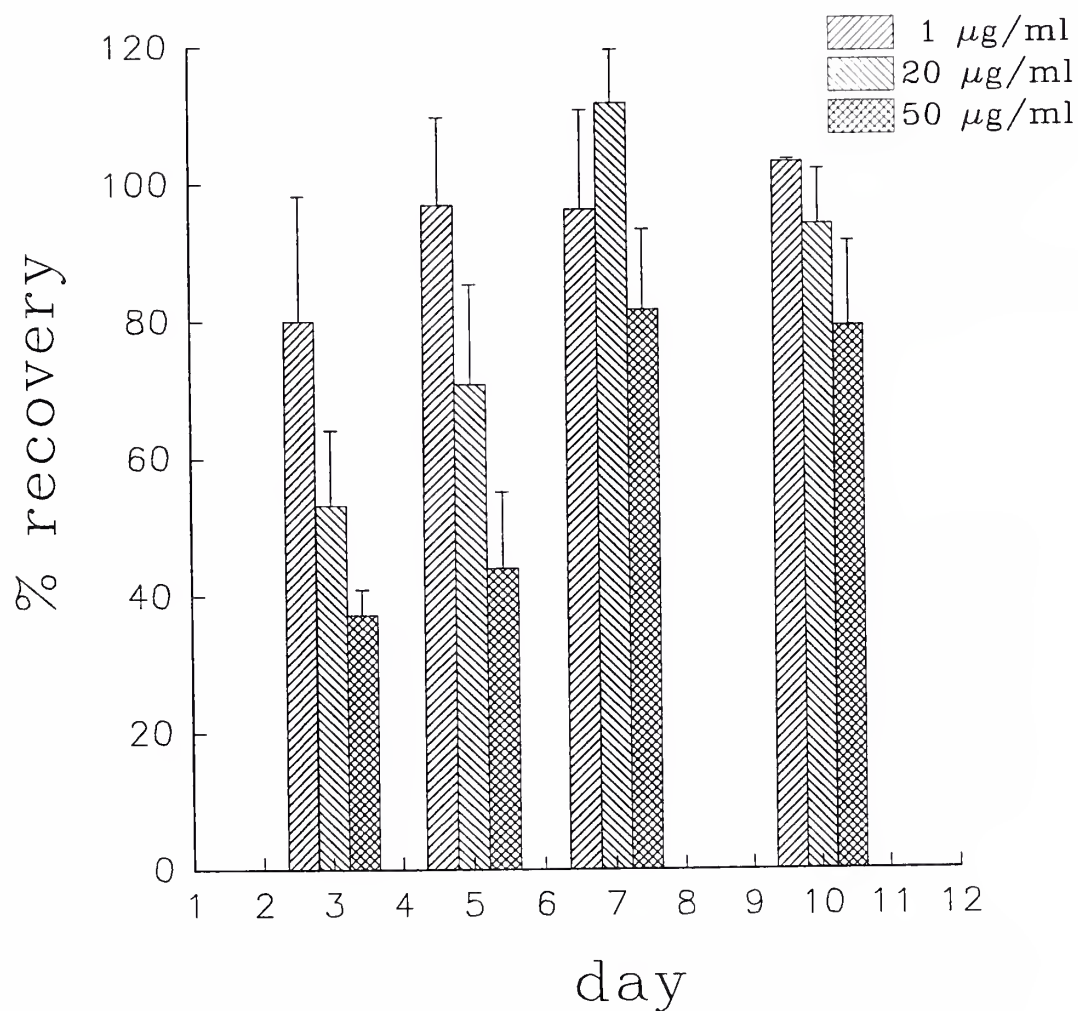


Figure 7-8. Summary graph of triplicate experiments performed on EC at 1, 20, and 50 $\mu\text{g}/\text{mL}$ 8-MOP. Percent recovery = number of treated cells/number of control cells. No effect is apparent at 1 $\mu\text{g}/\text{mL}$ 8-MOP. Inhibition with rapid recovery of EC proliferation is seen at both 20 and 50 $\mu\text{g}/\text{mL}$ 8-MOP.

Cell Migration

Figure 7-9 demonstrates SMC migration on day 3 following treatment with 0, 1, 20, and 50 $\mu\text{g}/\text{mL}$ 8-MOP. The photographs reveal that no concentration of 8-MOP was capable of producing an inhibitory effect on SMC migration. Studies on EC also demonstrated a lack of effect on cell migration, even at highest dose (data not shown). The extent of migration observed in cells treated with mitomycin did not differ significantly from that of cells not treated with mitomycin.

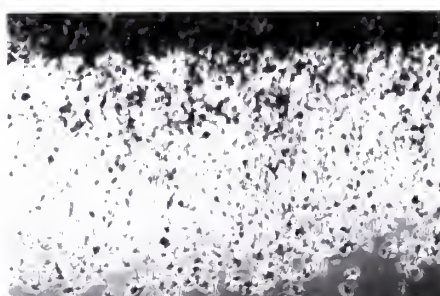
SMC Migration



0 $\mu\text{g}/\text{ml}$



1 $\mu\text{g}/\text{ml}$



20 $\mu\text{g}/\text{ml}$



50 $\mu\text{g}/\text{ml}$

Figure 7-9. Extent of SMC migration seen on day 3 after treatment with 0, 1, 20, and 50 $\mu\text{g}/\text{mL}$ 8-MOP and 12 J/cm^2 447 nm light. No difference is apparent among these cells treated at different 8-MOP concentrations.

Cell Morphology

Figures 7-10, 7-11, and 7-12 represent a series of photographs which depict the morphology of treated and control SMC at days 5, 7, and 10. The photographs reveal cell densities consistent with those expected based on the SMC proliferation data. The majority of cells in all samples appeared healthy. While no difference in morphology was appreciated between cells treated with 1 $\mu\text{g}/\text{mL}$ 8-MOP and control cells (Figure 7-10), morphologic examination of cells treated at 20 and 50 $\mu\text{g}/\text{mL}$ 8-MOP revealed cells which were larger and phenotypically different from their respective controls (Figures 7-11 and 7-12). Additionally, this difference in morphology appeared to resolve over time in cells treated with 20 $\mu\text{g}/\text{mL}$ 8-MOP (Figure 7-11) but not in those treated with 50 $\mu\text{g}/\text{mL}$ 8-MOP (Figure 7-12).

1 $\mu\text{g}/\text{ml}$ 8-MOP

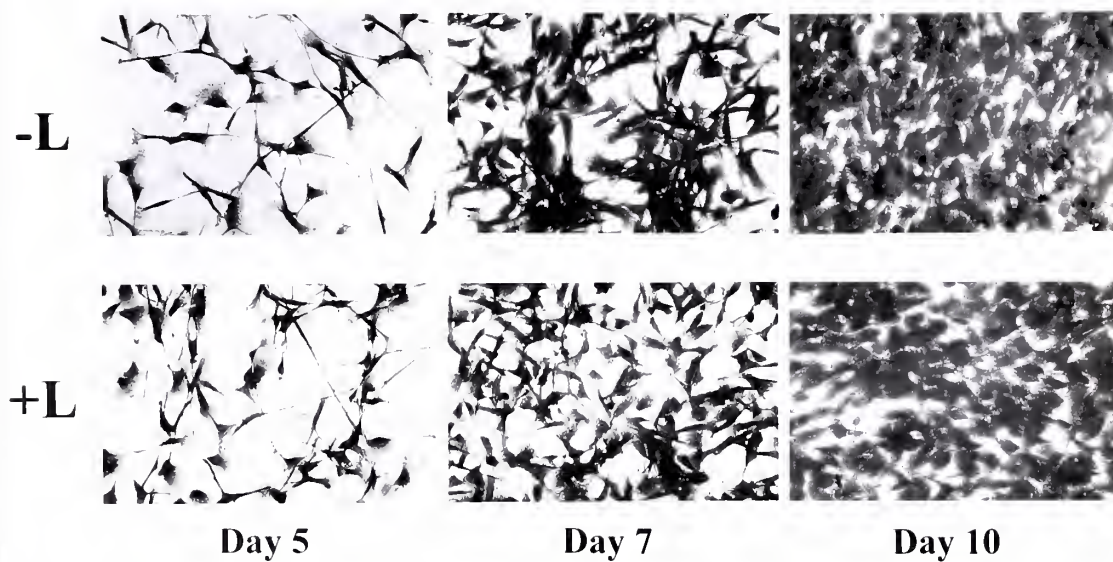


Figure 7-10. SMC morphology on days 5, 7, and 10 following treatment with 1 $\mu\text{g}/\text{mL}$ 8-MOP. Cell densities are consistent with those expected based on SMC proliferation data. No difference in morphology is appreciable between control and treated cells.

20 $\mu\text{g/ml}$ 8-MOP

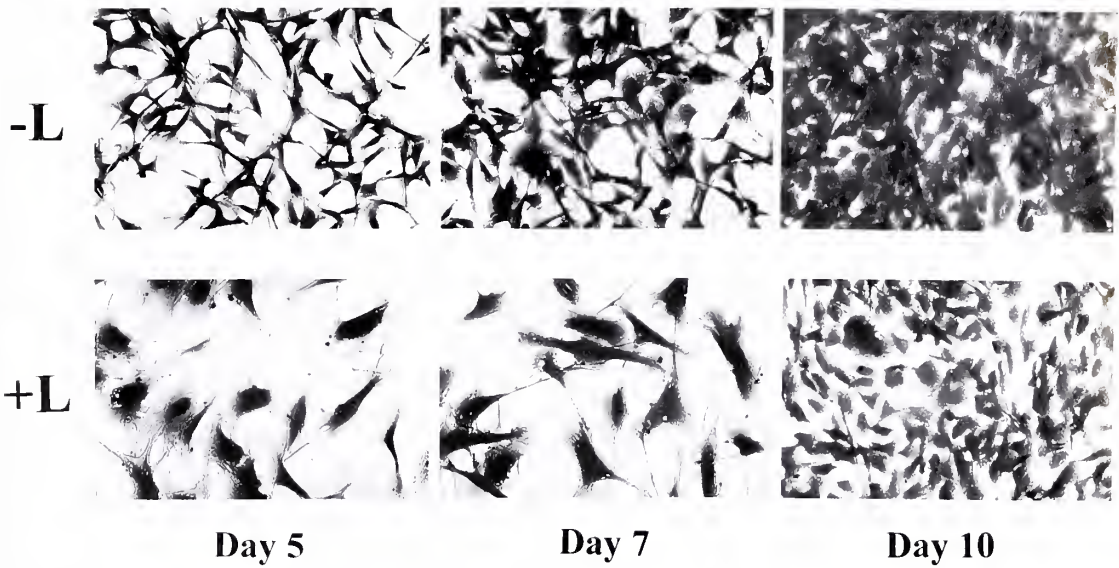


Figure 7-11. SMC morphology on days 5, 7, and 10 following treatment with 20 $\mu\text{g/mL}$ 8-MOP. Cell densities are consistent with those expected based on SMC proliferation data. Treated cells appear larger and phenotypically different from control cells on day 5. This difference in morphology appears to begin to resolve by day 10.

50 $\mu\text{g/ml}$ 8-MOP

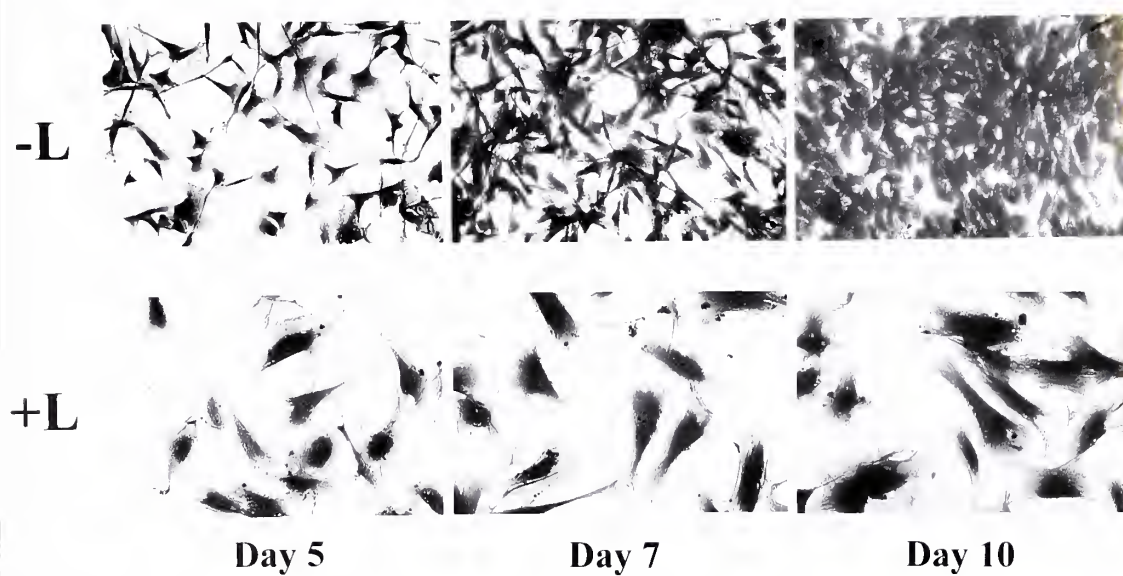


Figure 7-12. SMC morphology on days 5, 7, and 10 following treatment with 50 $\mu\text{g/mL}$ 8-MOP. Cell densities are consistent with those expected based on SMC proliferation data. Treated cells appear larger and phenotypically different from control cells on day 5. This difference in morphology appears to persist.

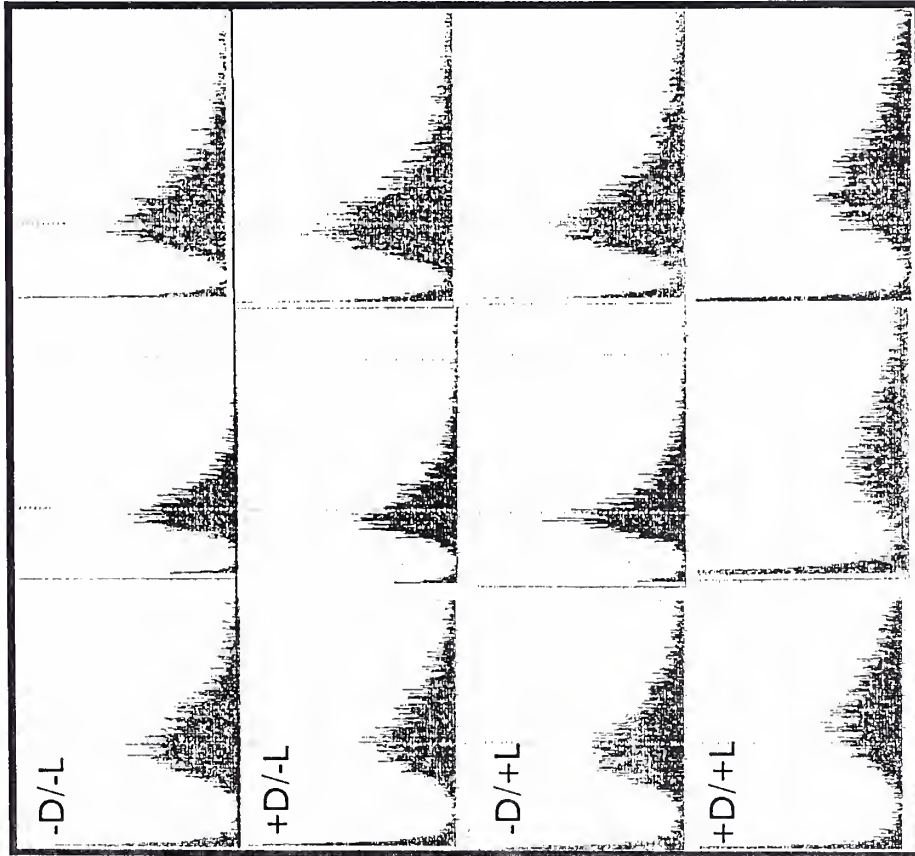
Cell Size

Figure 7-13 shows a series of size distribution diagrams. The x-axis corresponds to the size of individual cells (measured in femtoliters, fL) while the y-axis represents the number of cells in each sample measured at that particular size. For each day, the size distribution for untreated control cells (-D/-L), 8-MOP only-treated control cells (+D/-L), visible light only-treated control cells (-D/+L), and cells treated with both 8-MOP and visible light (+D/+L) are shown. At any given day, the vertical dotted line represents the average (mode) size of the three different groups of control cells.

On day 3, the average size of untreated SMC was 1.70 fL, while the average size of untreated EC was 1.32 fL. For both SMC and EC, treatment with either 8-MOP or visible light alone failed to induce any significant change in cell size. Treatment with both 8-MOP and visible light, on the other hand, resulted in an increase in average cell size. This increase in cell size was maintained in SMC over the time course studied, with only a slight decrease in cell size detected by day 14. The increase in EC size, however, rapidly resolved with a return to control sizes by day 10.

These changes in cell size were plotted over a time course (Figure 7-14). For SMC, average cell size increased to 2.50 fL by day 5 and then plateaued at 3.20 fL by day 10. A different pattern was observed in EC, which increased in average size to 3.80 fL by day 5 but returned to near control size (1.30 fL) by day 10.

Figure 7-13. Cell size distribution diagrams. x-axis = size of cells, measured in femtoliters (fL); y-axis = number of cells measured at the given size. D = drug; L = light. The four rows represent size distribution diagrams for untreated control cells (-D/-L), 8-MOP only-treated control cells (+D/-L), visible light only-treated control cells (-D/+L), and 8-MOP and visible light-treated cells (+D/+L). The vertical dotted line represents the average (mode) size of the three different groups of control cells.

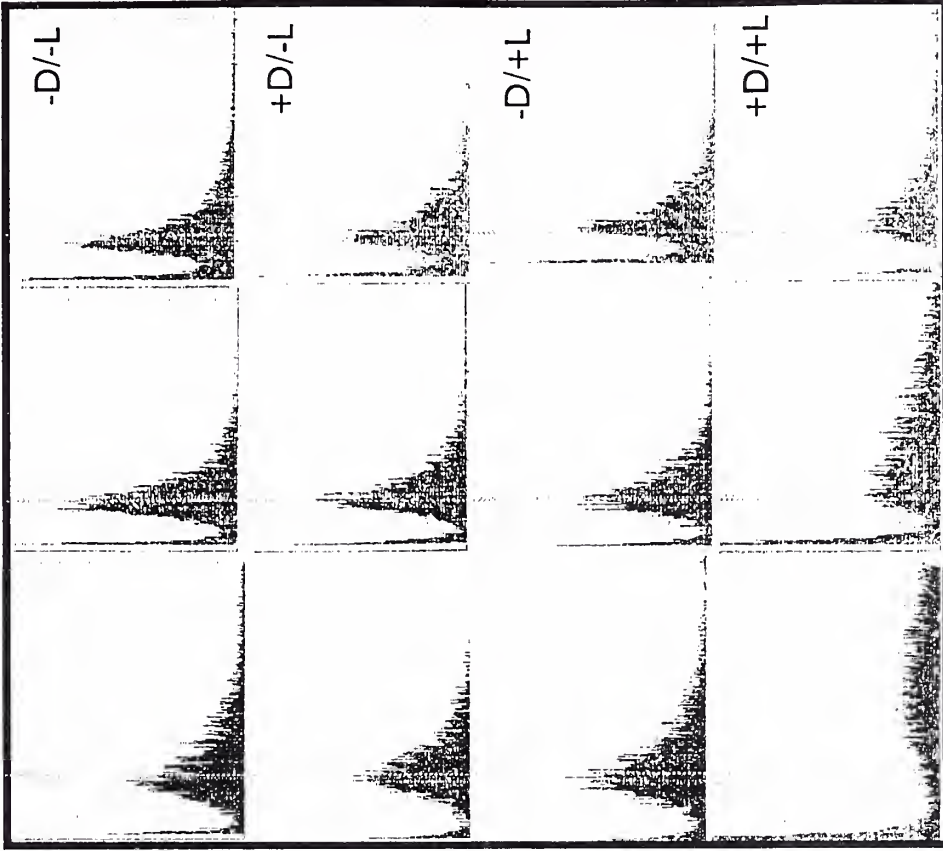


DAY 3

DAY 7
10

DAY

SMC



DAY 3

DAY 7
10

DAY

EC

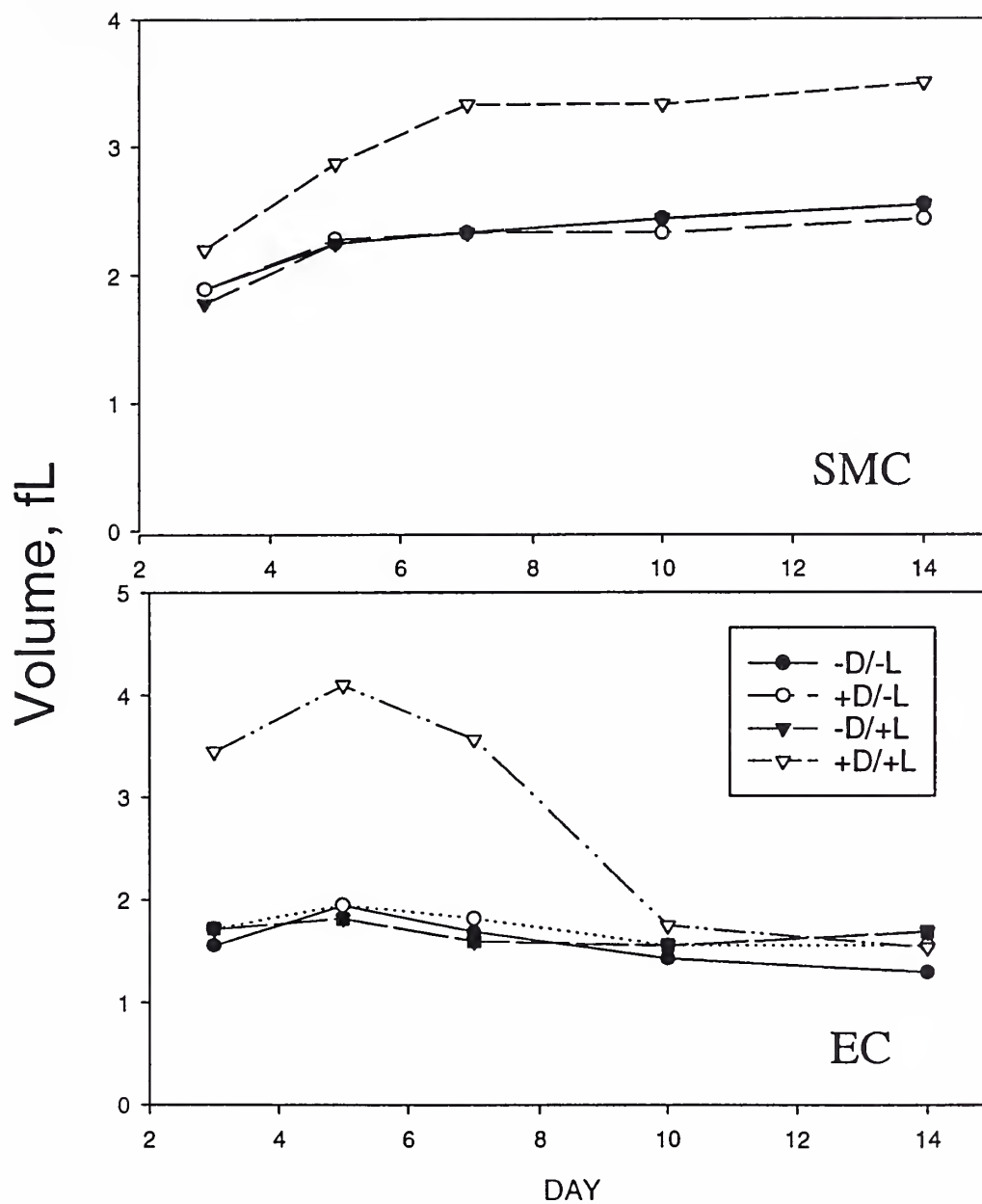


Figure 7-14. Changes in cell size (volume) followed over the course of 14 days. Average cell size appears to increase and plateau in SMC treated with both drug and light (clear triangles). In EC treated with both drug and light, average cell size initially increases but rapidly returns to control sizes by day 10 (clear triangles).

Photoadduct Formation

SMC and EC treated with 20 $\mu\text{g}/\text{mL}$ 8-MOP and 32 J/cm^2 447 nm light revealed comparable levels of photoadduct formation. 110 adducts per million base pairs were found in SMC, while 200 adducts per million base pairs were seen in EC. Relative formation of the different types of photoadducts (4', 5'-monoadducts; 3, 4-monoadducts; and crosslinks) were similar between the two cell types as demonstrated in the following high-performance liquid chromatography (HPLC) curves (Figure 7-15).

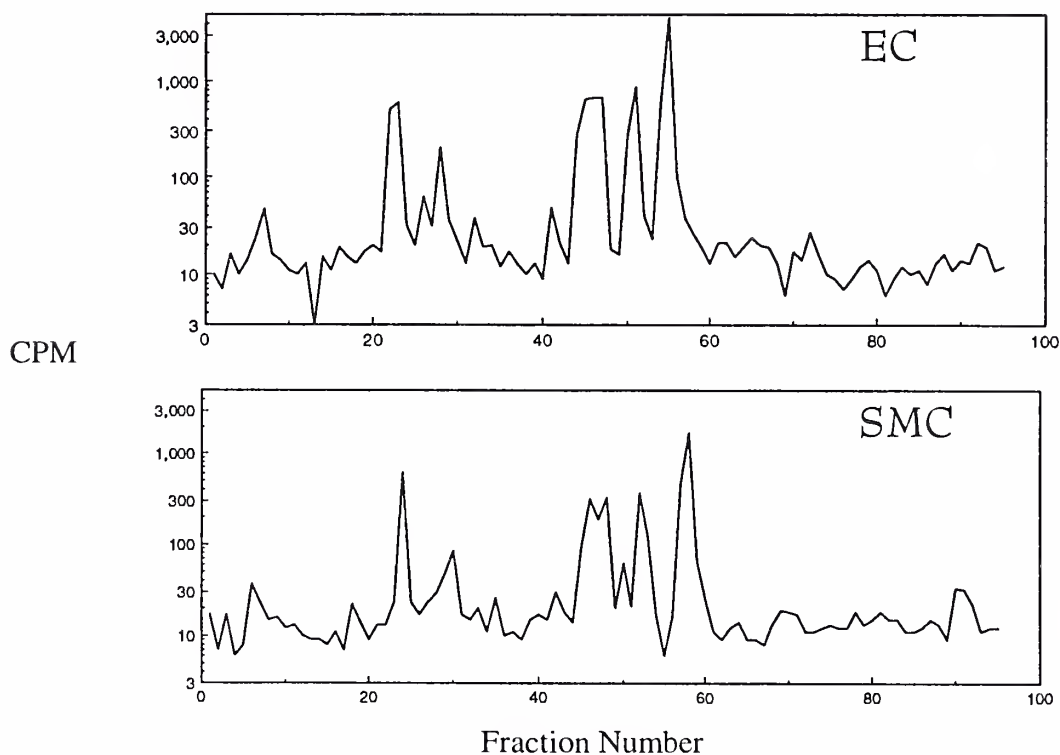


Figure 7-15. Graphs comparing photoadduct formation in EC and SMC. CPM = counts per minute. Late-eluting 8-MOP-thymidine photoadducts were detected by liquid scintillation analysis. Photoadduct distributions between the two cell types were similar.

8. Discussion

Discussion of Results

Cell Proliferation. The present study demonstrates that 8-MOP photoactivated with 447 nm visible light can reversibly inhibit both SMC and EC proliferation *in vitro* in a dose-dependent fashion. The study also reveals that different 8-MOP dosages cause a range of effects in SMC proliferation, from no effect to reversible cytostasis to cytotoxicity. These selected dosages appear to have significantly attenuated effects on EC compared to SMC.

The rapidly reversible inhibition of EC proliferation observed in the experiments, even at high 8-MOP concentrations, bears clinical significance in light of previous studies which have demonstrated that a functionally intact endothelium contributes to the inhibition of SMC proliferation (Ip et al., 1991). The fact that photochemotherapy with 8-MOP and visible light can selectively inhibit SMC proliferation without causing damage to EC immediately suggests this treatment regimen as a potential solution to the problem of post-angioplasty restenosis.

Cell Migration. As intimal hyperplasia involves not only SMC proliferation but also SMC migration, experiments evaluating the effects of 8-MOP photoactivated with 447 nm visible light on cell migration were performed. Unlike the effects observed in SMC and EC proliferation, however, no inhibition of either SMC or EC migration was found. Nevertheless, while both SMC migration and proliferation are involved in the neointima

formation which occurs after angioplasty, it is known that SMC proliferation contributes more materially to the process.

It has been estimated that only about one half of the SMC which migrate into the intima after angioplasty undergo further proliferation. The remaining SMC do not. Those SMC which do continue to proliferate undergo approximately three rounds of division, thereby constituting eight ninths of the final neointimal cell population (Clowes and Schwartz, 1985). This suggests that SMC proliferation has a significantly greater impact on restenosis than SMC migration; hence, the finding that phototherapy with 8-MOP and visible light fails to inhibit cell migration does not disqualify this treatment regimen as a potential solution to the problem of post-angioplasty restenosis.

Cell Morphology. Despite its lack of effect on cell migration, the combination of 8-MOP and visible light was found to affect SMC morphology. It is interesting to note that just as different effects in SMC proliferation were observed in response to different 8-MOP dosages, a range of effects in SMC morphology was also seen in response to different 8-MOP dosages. While no morphological differences were appreciated between SMC treated with 1 $\mu\text{g}/\text{mL}$ 8-MOP and their controls, SMC treated with 20 $\mu\text{g}/\text{mL}$ and 50 $\mu\text{g}/\text{mL}$ 8-MOP appeared larger and phenotypically different from their respective controls. Moreover, this difference in morphology appeared to resolve over time in the cells treated with 20 $\mu\text{g}/\text{mL}$ 8-MOP but not in those treated with 50 $\mu\text{g}/\text{mL}$. Whether this

range of effects observed in cell morphology is somehow related to the range of effects seen in SMC proliferation remains to be elucidated.

Cell Size. Additional studies employing a Channelyzer capable of measuring cell sizes (volumes) were conducted to corroborate the cell enlargement induced by treatments with 8-MOP and 447 nm visible light observed in the morphology experiments. Cell size measurements confirmed that treatment with 20 $\mu\text{g}/\text{mL}$ 8-MOP causes an increase in average cell size for both SMC and EC. Unlike the findings noted in the morphology studies, however, the increase in SMC sizes did not resolve over time but instead persisted. The increase in EC sizes, on the other hand, appeared to resolve by day 10.

The reason for these differences in cell size changes over time noted between the morphology experiments and cell size experiments is unclear but may be due to the fact that morphology studies assess cell sizes on a two-dimensional level, while a Channelyzer measures cell sizes in three dimensions. The difference in ability of SMC and EC to return to control sizes following the same treatment represents an important finding and may be related to the differences observed in the cell proliferation experiments, as an attenuated response to treatment with the same 8-MOP dosage is again observed in EC compared to SMC.

Photoadduct formation. As anticipated, the number of photoadducts measured in SMC and EC were within the same order of magnitude. Given the comparatively attenuated effects of the treatments on EC proliferation and size, one might have expected fewer photoadducts to have been found in EC than SMC. Surprisingly, the number of

photoadducts measured in EC was nearly twice that measured in SMC. This suggests that the attenuated effects observed in EC are not the result of the formation of fewer photoadducts.

Potential Future Experiments

Comparison between SMC and EC proliferation curves reveals that photochemotherapy with high doses of 8-MOP is cytotoxic to SMC but yields only transient cytostasis in EC. The reason for these differences in response between SMC and EC to identical photochemotherapeutic treatments remains to be determined. As it had been presumed that inhibition of cellular proliferation could be directly related to extent photoadduct formation, the decreased sensitivity of EC to 8-MOP treatments was initially hypothesized to be the result of decreased photoadduct formation. The preliminary study on photoadduct formation, however, revealed that EC forms nearly twice the number of photoadducts as SMC.

As this observation is based on a single experiment, repeat experiments on photoadduct formation are in order. Repeat studies may confirm that photoadduct formation is indeed consistently greater in EC or may reveal that the difference in photoadduct formation between SMC and EC observed in the pilot study falls within normal variance.

Assuming that the greater photoadduct formation observed in EC is genuine, experiments designed to explicate the fact that EC are less sensitive to treatments with 8-MOP and visible light despite more extensive photoadduct formation should be undertaken. As differences in DNA repair rates which would allow EC to restore its proliferative

functionality more rapidly than SMC might account for this discrepancy, experiments comparing photoadduct formation levels in SMC and EC over a time course could be performed. These studies would help to characterize the DNA repair kinetics of the two cell types and might reveal differences. Specifically, they might demonstrate that EC possess more efficient DNA repair machinery than SMC.

However, should these experiments reveal that EC exhibit greater photoadduct formation than SMC at all time points, the hypothesis that inhibition of cell proliferation is directly related to extent photoadduct formation would have to be challenged. Further experimentation might reveal that extent photoadduct formation is only one of a number of factors which contribute to the inhibition of cell proliferation.

Another issue which could potentially be addressed in future experiments is the question of whether photochemotherapy with 8-MOP and visible light would yield similar results in human coronary cells. The difference in response seen between bovine aortic SMC and EC already suggests that dissimilar cell types may respond differently to the same treatment. Thus, studies performed on human coronary cells *in vitro* would be useful.

While photochemotherapy with 8-MOP and visible light has been shown to dose-dependently inhibit proliferation of SMC and EC *in vitro*, it would also be valuable to evaluate the effects of this treatment regimen on vascular cells *in vivo*. The experimental methods employed in the present study artificially isolate SMC from EC. Recall that in the normal coronary artery, these cells are separated by only a thin, fenestrated internal elastic membrane (see “The Normal Coronary Artery,” Chapter 1). Thus, in the live

model, these cells interact with each other and affect one another's functional capacities. Hence, *in vivo* studies designed to corroborate the beneficial effects of phototherapy with 8-MOP suggested by our *in vitro* experiments would also prove useful.

Finally, studies examining the effects of visible light-activated 8-MOP on cell functions other than proliferation and migration might prove beneficial. For example, experiments designed to assess the effects of these treatment regimens on the ability of SMC and EC to synthesize proteins could be performed. If protein synthesis were inhibited, follow-up studies could be performed to assess recovery of synthetic function. These types of experiments on the effects of visible light-activated 8-MOP on vascular cell function would further elucidate the suitability of this treatment modality for clinical trials.

Significance of Results

The clinical significance of the present study is related to the established long-term safety of 8-MOP, the availability of 447 nm lasers, the ability to target therapy to the angioplasty site, and the potentially reversible nature of the effects of therapy.

As mentioned previously, 8-MOP exhibits a rapid clearance which results in minimal clinical phototoxicity. Its common use in the treatment of dermatologic diseases has established its long-term safety. Moreover, the significant reduction in extent of crosslink formation seen at photoactivation with 447 nm light may render photochemotherapy with 8-MOP at this wavelength a greater therapeutic index.

Perhaps this reduction in crosslink formation contributes to the rapidity of the proliferative functional recovery observed in SMC treated with intermediate dose (20 $\mu\text{g}/\text{mL}$) 8-MOP. The cytostatic effect of this treatment regimen without cytotoxicity represents a theoretical advantage over cytotoxic therapies for the prevention of restenosis. SMC necrosis caused by cytotoxic therapies could compromise the mechanical integrity of the arterial wall and result in the formation of an aneurysm. Moreover, cytokines released by damaged or dying SMC could stimulate a secondary local inflammatory response and cause an exacerbation of the cellular proliferative response (Sumpio et al., 1994).

As the migration and proliferation of SMC stimulated by angioplasty begins as early as 24 to 48 hours after the procedure and lasts for approximately one week (Forrester et al., 1991; Ip et al., 1991), a transient, reversible inhibition of SMC proliferation may represent an optimal solution to the problem of post-angioplasty restenosis. The present study demonstrates that 8-MOP photoactivated with visible light is capable of inhibiting SMC proliferation, presumably via photoadduct formation. Excision of these photoadducts by DNA repair mechanisms would allow for the eventual return of proliferative capacity and could result in the restoration of SMC functionality at a time when the stimulus to proliferate has waned.

Currently available technology permits photochemotherapy with 8-MOP and visible light to be directed to a discrete site on the vessel wall by means of local drug and/or light delivery. While 8-MOP has traditionally been administered systemically (both orally and

intravenously) for other therapeutic applications, high local concentrations of the drug could be attained via intra-arterial administration with a double-balloon catheter.

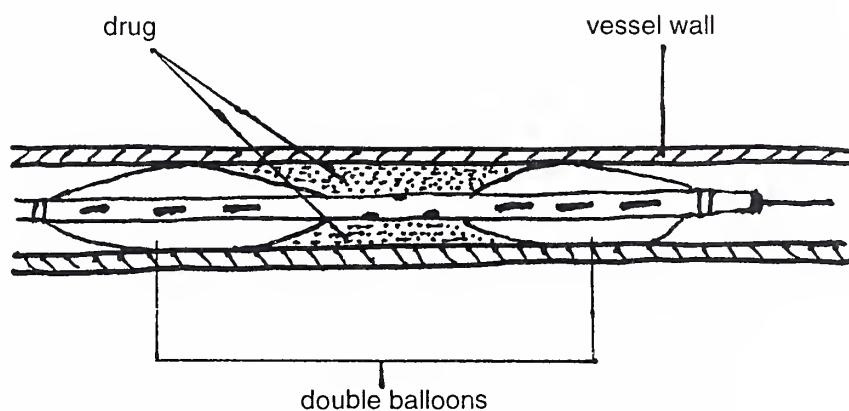


Figure 8-1. Schematic of a double-balloon catheter demonstrating how high local concentrations of drug could be achieved with this device.

Intra-arterial light irradiation of a segment of the vessel wall could then be achieved using a recently described fiber-optic balloon catheter, which has been clinically evaluated for simultaneous balloon dilatation and arterial wall irradiation (Spears et al., 1990).

9. Conclusion

In conclusion, SMC proliferation constitutes a major mechanism by which restenosis after angioplasty occurs. A therapeutic regimen capable of inhibiting SMC proliferation both selectively and reversibly might represent an ideal solution to the problem of post-angioplasty restenosis. As the present study demonstrates that photochemotherapy with 8-MOP and visible light possesses these characteristics, this treatment regimen may represent a novel approach to the prevention of post-angioplasty restenosis.

10. References

1. Austin GE, Ratliff NB, Hollman J, Tabei S, Phillips DF. Intimal proliferation of smooth muscle cells as an explanation for recurrent coronary artery stenosis after percutaneous transluminal coronary angioplasty. *J Am Coll Cardiol* 6: 369-375 (1985).
2. Barath P, Arakawa K, Cao J, Fishbein M, Fagin J, Lusis A, Forrester J. Low dose of antitumor agents prevents smooth muscle cell proliferation after endothelial injury (abstract). *J Am Coll Cardiol* 13:252A (1989).
3. Bates ER, McGillem MJ, Mickelson JK, Pitt B, Mancini J. A monoclonal antibody to the platelet receptor GPIIb/IIIa (7E3) prevents acute thrombosis in a canine model of coronary angioplasty (abstract). *Circulation* 78 (Suppl. II):289 (1988).
4. Bertrand ME, Lablanche JM, Fourrier JL, Gommeaux A, Ruel M. Relation of restenosis after percutaneous transluminal coronary angioplasty to vasomotion of the dilated coronary arterial segment. *Am J Cardiol* 63:277-281 (1989).
5. Bevilacqua PM, Edelson RL, Gasparro FP. High performance liquid chromatography analysis of 8-methoxypsoralen monoadducts and crosslinks in lymphocytes and keratinocytes. *J Invest Dermatol* 97:151-155 (1991).
6. Bilazarian SD, Currier JW, Haudenschild CC, Heyman D, Powell J, Ryan TJ, Faxon DP. Angiotensin converting enzyme inhibition reduces restenosis in experimental angioplasty (abstract). *J Am Coll Cardiol* 17:268A (1991).
7. Brickl R, Schmid J, Koss FW. Clinical pharmacology of oral psoralen drugs. *Photodermatology* 1: 174-186 (1984).
8. Califf RM. Restenosis: the cost to society. *Am Heart J* 130:680-684 (1995).
9. Castellot JJ Jr., Addonizio ML, Rosenberg R, Karnowsky MJ. Cultured endothelial cells produce a heparin-like inhibitor of smooth muscle cell growth. *J Cell Biol* 90: 372-377 (1981).
10. Chesebro JH, Webster MWI, Reeder GS, Mock MB, Grill DE, Bailey KR, Steichen S, Fuster V. Coronary angioplasty: antiplatelet therapy reduces acute complications but not restenosis (abstract). *Circulation* 80 (Suppl. II):64 (1989).
11. Clinton SK, Libby P. Cytokines and growth factors in atherogenesis. *Arch Pathol & Lab Med* 116: 1292- 1300 (1992).
12. Clowes AW, Karnowsky MJ. Suppression by heparin of smooth muscle cell proliferation in injured arteries. *Nature* 265: 625-626 (1977).

13. Clowes A, Schwartz S. Significance of quiescent smooth muscle migration in the injured rat carotid artery. *Circ Res* 56: 139-145 (1985).
14. Cundari E, Averbek D. 8-methoxypsoralen-photoinduced DNA Cross-links as determined in yeast by alkaline step elution under different reirradiation conditions. Relation with genetic effects. *Photochem Photobiol* 48:315-320 (1988).
15. Currier JW, Pow TK, Minihan AC, Haudenschild CC, Faxon DP, Ryan TJ. Colchicine inhibits restenosis after iliac angioplasty in the atherosclerotic rabbit (abstract). *Circulation* 80 (Suppl. II):66 (1989).
16. Dartsch PC, Ischinger T, Betz E. Differential effect of photofrin II on growth of human smooth muscle cells from nonatherosclerotic arteries and atheromatous plaques in vitro. *Arteriosclerosis* 10: 616-624 (1990).
17. Dartsch PC, Ischinger T, Betz E. Response of cultured smooth muscle cells from human nonatherosclerotic arteries and primary stenosing lesions after photoradiation: Implications for photodynamic therapy of vascular stenoses. *J Am Coll Cardiol* 15: 1545-1550 (1990).
18. Davies MJ, Thomas A. Thrombosis and acute coronary-artery lesions in sudden cardiac ischemic death. *N Engl J Med* 310:1137-1140 (1984).
19. Deckelbaum LI, Scott JJ, Stetz ML, O'Brien KM, Sumpio BE, Madri JA, Bell L. Photoinhibition of smooth muscle cell migration: potential therapy for restenosis. *Lasers in Surg & Med* 13:4-11 (1993).
20. Edwards WD. Atherosclerotic plaques: natural and unnatural history. In: *Cardiovascular pathology: clinicopathologic correlations and pathogenetic mechanisms*. Schoen FJ and Gimbrone MA Jr., eds. Williams & Wilkins, Philadelphia (1995).
21. Ellis SG, Roubin GS, Wilentz J, Douglas JS Jr, King SB III. Effect of 18- to 24-hour heparin administration for prevention of restenosis after uncomplicated coronary angioplasty. *Am Heart J* 117:777-782 (1989).
22. Eton D, Coburn MD, Shim V, Panek W, Lee DA, Moore WS, Ahn SS. Inhibition of intimal hyperplasia by photodynamic therapy using photofrin. *J Surg Res* 53: 558-562 (1992).
23. Faxon DP, Currier JW. Prevention of Post-PTCA Restenosis. *Ann N Y Acad Sci* 748:419-427 (1995).
24. Faxon DP & the MARCATOR INVESTIGATORS. Angiotensin converting enzyme inhibition and restenosis: the final results of the MARCATOR study (abstract). *Circulation* 86 (Suppl. I):53 (1992).
25. Faxon DP, Sanborn TA, Haudenschild CC, Ryan TJ. Effect of antiplatelet therapy on restenosis after experimental angioplasty. *Am J Cardiol* 53:72C-76C (1984).
26. Faxon DP, Spiro T, Minor S, Douglas J, Cote G, Dorosti K, Gottlieb R, Califf R, Topol E, Gordon J. Enoxaparin, a low molecular weight heparin, in the prevention of restenosis after angioplasty: results of a double blind randomized trial (Abstract). *J Am Coll Cardiol* 19:258A (1992).
27. Forrester JS, Fishbein M, Helfant R, Fagin J. A paradigm for restenosis based on cell biology: Clues for the development of new preventive therapies. *J Am Coll Cardiol* 17: 758-769 (1991).
28. Fox PL, DiCorleto PE. Fish oils inhibit endothelial cell production of platelet-derived growth factor-like protein. *Science* 241:453-456 (1988).

29. Franklin SM, Faxon DP. Pharmacologic prevention of restenosis after coronary angioplasty: review of the randomized clinical trials. *Coronary Artery Dis* 4:232-242 (1993).
30. Friedman RJ, Stemerman MB, Wenz B, Moore S, Gauldie J, Gent M, Tiell ML, Spaet TH. The effect of thrombocytopenia on experimental arteriosclerotic lesion formation in rabbit. *J Clin Invest* 60:1191-1201 (1977).
31. Gasparro FP. *Extracorporeal Photochemotherapy: Clinical Aspects and the Molecular Basis for Efficacy*. R.G. Landes Company, Austin (1994).
32. Gasparro F, ed. Psoralen-DNA interactions: thermodynamics and photochemistry. In: *Psoralen DNA Photobiology, vol. I*. CRC press, Boca Raton (1988).
33. Gasparro F, Bevilacqua P, Goldminz D, Edelson R. Repair of 8-MOP photoadducts in human lymphocytes. In: *DNA Damage and Repair in Human Tissues*, pp. 137-148. Sutherland BM and Woodhead AD, eds. Plenum Press, New York (1990).
34. Gasparro FP, Gattolin P, Olack GA, Deckelbaum LI, Sumpio BE. The excitation of 8-methoxypsoralen with visible light: reversed phase HPLC quantitation of monoadducts and cross-links. *Photochem Photobiol* 57: 1007-1010 (1993).
35. Gellman, J, Ezekowitz MD, Sarembock IJ, Azrin MA, Nochomowitz LE, Lerner E, Haudenschild CC. Effect of lovastatin on intimal hyperplasia after balloon angioplasty: a study in an atherosclerotic hypercholesterolemic rabbit. *J Am Coll Cardiol* 17:251-259 (1991).
36. Gordon JB, Berk BC, Bettman MA, Selwyn AP, Rennke H, Alexander RW. Vascular smooth muscle cell proliferation is synergistically inhibited by low molecular weight heparin and hydrocortisone (abstract). *Circulation* 76 (Suppl. IV):213 (1987).
37. Gruentzig AR, Senning A, Siefenthaler WE. Nonoperative dilation of coronary-artery stenosis. *N Engl J Med* 301:61-68 (1979).
38. Gupta AK, Anderson TF. Psoralen photochemotherapy. *J Am Acad Dermatol* 17: 703-734 (1987).
39. Hanasaki K, Nakano T, Arita H. Receptor-mediated mitogenic effect of thromboxane A2 in vascular smooth muscle cells. *Biochem Pharm* 40:2535-2542 (1990).
40. Hanke H, Strohschneider T, Oberhoff M, Betz E, Karsch KR. Time course of smooth muscle cell proliferation in the intima and media of arteries following experimental angioplasty. *Circ Res* 67: 651-659 (1990).
41. Hermans WRM, Rensing BJ, Strauss BH, Serruys PW. Prevention of restenosis after percutaneous transluminal coronary angioplasty: The search for a "magic bullet." *Amer Heart J* 122: 171-187 (1991).
42. Herrman JP, Hermans WR, Vos J, Serruys PW. Pharmacological approaches to the prevention of restenosis following angioplasty. The search for the Holy Grail? (Part I). *Drugs* 46:18-52 (1993).
43. Ip JH, Fuster V, Israel D, Badimon L, Badimon J, Chesebro JH. The role of platelets, thrombin and hyperplasia in restenosis after coronary angioplasty. *J Amer Coll Cardiol* 17: 77B-88B (1991).

44. Ip JH, Fuster V, Israel D, Badimon L, Badimon J, Taubman MB, Chesebro JH. Syndromes of accelerated atherosclerosis: Role of vascular injury and smooth muscle cell proliferation. *J Am Coll Cardiol* 15: 1667-1687 (1990).
45. Jenkins RD, Sinclair IN, Leonard BM, Sandor T, Schoen FJ, Spears JR. Laser balloon angioplasty versus balloon angioplasty in normal rabbit iliac arteries. *Lasers in Surg Med* 9: 237-247 (1989).
46. Knudtson ML, Flintoft VF, Roth DL, Hansen JL, Duff HJ. Effect of short-term prostacyclin administration on restenosis after percutaneous transluminal coronary angioplasty. *J Am Coll Cardiol* 15:691-697 (1990).
47. Kuntz RE, Gibson, CM, Nobuyoshi M, Baim DS. Generalized Model of restenosis after conventional balloon angioplasty, stenting and directional atherectomy. *J Am Coll Cardiol* 21: 15-25 (1993).
48. LaMuralgia GM, ChandraSekar NR, Flotte TJ, Abbott WM, Michaud N, Hasan T. Photodynamic therapy inhibition of experimental hyperplasia: acute and chronic effects. *J Vasc Surg* 19: 321-331 (1994).
49. Lange RA, Willard JE, Hillis, LD. Southwestern internal medicine conference: Restenosis: the Achilles heel of coronary angioplasty. *Am J Med Sci* 306:265-275 (1993).
50. Libby P. Do vascular wall cytokines promote atherogenesis? *Hosp Prac* 27 (10):51-58 (1992).
51. Litvack F, Grundfest WS, Forrester JS, Fishbein MC, Swan HJC, Corday E, Rider DM, McDermid IS, Pacala TJ, Laudenslager JB. Effects of hematoporphyrin derivative and photodynamic therapy on atherosclerotic rabbits. *Am J Cardiol* 56: 667-671 (1985).
52. Liu MW, Roubin GS, King SB. Restenosis after coronary angioplasty: Potential biologic determinants and role of intimal hyperplasia. *Circulation* 79: 1374-1387 (1989).
53. Liu MW, Roubin GS, Robinson KA, Black AJR, Hearn JA, Siegel RJ, King SB III. Trapidil in preventing restenosis after balloon angioplasty in the atherosclerotic rabbit. *Circulation* 81:1089-1093 (1990).
54. Lovqvist A, Emanuelsson H, Nilsson J, Lundqvist H, Carlsson J. Pathophysiological mechanisms for restenosis following coronary angioplasty: possible preventive alternatives. *J Intern Med* 233:215-226 (1993).
55. Lundergan CF, Foegh ML, Ramwell PG. Peptide inhibition of myointimal proliferation by angiopeptin, a somatostatin analogue. *J Am Coll Cardiol* 17:132B-136B (1991).
56. March KL, Patton BL, Wilensky RL, Hathaway DR. 8-Methoxypsoralen and longwave ultraviolet irradiation are a cell cycle-independent antiproliferative combination for vascular smooth muscle. *J Am Coll Cardiol* 19: 164A (1992).
57. March KL, Patton BL, Wilensky RL, Hathaway DR. 8-Methoxypsoralen and longwave ultraviolet irradiation are a novel antiproliferative combination for vascular smooth muscle. *Circulation* 87: 184-191 (1993).
58. MERCATOR STUDY GROUP. Does the new angiotensin converting enzyme inhibitor cilazapril prevent restenosis after percutaneous transluminal coronary angioplasty. Results of the MERCATOR study: a multicenter, randomized, double-blind placebo-controlled trial. *Circulation* 86:100-110 (1992).

59. Muller DWM, Topol EJ, Abrams GD, Gallagher KP, Ellis SG. Intramural methotrexate therapy for the prevention of neointimal thickening after balloon angioplasty. *J Am Coll Cardiol* 20: 460-466 (1992).
60. MULTICENTER ITALIAN RESEARCH TRIAL WITH TRAPIDIL IN THE PREVENTION OF CORONARY RESTENOSIS AFTER PTCA (STARC). Trapidil (platelet derived growth factor inhibitor) prevents restenosis after PTCA: results of the STARC Study (Abstract). *Eur Heart J* 14:277 (1993).
61. Nobuyoshi M, Kimura T, Ohishi H, Horiuchi H, Nosaka H, Hamasaki N, Yokoi H, Kim K. Restenosis after percutaneous transluminal coronary angioplasty: Pathologic observations in 20 patients. *J Am Coll Cardiol* 17:433-439 (1991).
62. Okamoto S, Masaaki I, Setsuda M, Konishi T, Nakano T. Effects of trapidil (triazolopyrimidine), a platelet-derived growth factor antagonist, in preventing restenosis after percutaneous transluminal coronary angioplasty. *Am Heart J* 123:1439-1444 (1992).
63. O'Keefe JH, Giorgi LV, Hartzler GO, Good TH, Ligon RW, Webb DL, McCallister BD. Effects of diltiazem on complications and restenosis after coronary angioplasty. *Am J Cardiol* 67:373-376 (1991).
64. O'Keefe JH Jr, McCallister BD, Bateman TM, Kuhnlein DL, Ligon RW, Hartzler GO. Ineffectiveness of colchicine for the prevention of restenosis after coronary angioplasty. *J Am Coll Cardiol* 19:1597-1600 (1992).
65. Olack GA, Gattolin P, Gasparro FP. Improved high performance liquid chromatographic analysis of 8-methoxypsoralen monoadducts and crosslinks in polynucleotide, DNA and cellular systems: analysis of split-dose protocols. *Photochem Photobiol* 57:941-949 (1993).
66. Ortu P, LaMuraglia GM, Roberts WG, Flotte TJ, Hasan T. Photodynamic therapy of arteries: A novel approach for treatment of experimental intimal hyperplasia. *Circulation* 85: 1189-1196 (1992).
67. Pepine CJ, Hirschfeld JW, Macdonald RG, Henderson MA, Bass TA, Goldberg S, Savage MP, Vetrovec G, Cowley M, Taussig AS, Whitworth HB, Margolis JR, Hill JA, Bove, AA, Jugo R, for the M-HEART Group. A controlled trial of corticosteroids to prevent restenosis after coronary angioplasty. *Circulation* 81:1753-1761 (1990).
68. Pow TK, Currier JW, Minihan AC, Haudenschild CC, Ryan TJ, Faxon, DP. Low molecular weight heparin reduces restenosis after experimental angioplasty (abstract). *Circulation* 80 (Suppl. II):64 (1989).
69. Preisack MB, Karsch KR. The paradigm of restenosis following percutaneous transluminal coronary angioplasty. *Eur Heart J* 14:187-192 (1993).
70. Raizner A, Hollman J, Demke D, Wakefield L and the Ciprostone investigators. Beneficial effects of ciprostone in PTCA: a multicenter, randomized, controlled trial (abstract). *Circulation* 78 (Suppl. II):290 (1988).
71. Rensing BJ, Hermans WRM, Beat KJ, Laarman GJ, Suryapranata H, Van Den Brand M, DeFeyter PJ, Serruys PW. Quantitative angiographic assessment of elastic recoil after percutaneous transluminal coronary angioplasty. *Am J Cardiol* 66:1039-1044 (1990).

72. Rensing BJ, Hermans WR, Deckers JW, et al. Lumen narrowing after percutaneous transluminal balloon angioplasty follows a near Gaussian distribution: a quantitative angiographic study in 1,445 successfully dilated lesions. *J Am Coll Cardiol* 19:939-945 (1992).
73. Roetlandts R. The history of photochemotherapy. *Photoderm, Photoimmunol & Photomed* 8: 184-189 (1991).
74. Ross R. Rous-Whipple Award Lecture: Atherosclerosis: A defense mechanism gone awry. *Am J Pathol* 143:987-1002 (1993).
75. Ross R. The pathogenesis of atherosclerosis: a perspective for the 1990s. *Nature* 362: 801-809 (1993).
76. Ross R, Glomset JA. Atherosclerosis and the arterial smooth muscle cell. *Science* 180:1332-1339 (1973).
77. Sahni R, Maniet AR, Voci G, Banka VS. Prevention of restenosis by lovastatin (abstract). *Circulation* 80 (Suppl. II):65 (1989).
78. Schwartz L, Bourassa MG, Lesperance J, Aldridge HE, Kazim F, Salvatori VA, Henderson M, Bonan R, David PR. Aspirin and dipyridamole in the prevention of restenosis after percutaneous transluminal coronary angioplasty. *N Engl J Med* 318:1714-1719 (1988).
79. Serruys PW, Luijten HE, Beatt KJ, Geuskens R, de Feyter PJ, van den Brand M, Reiber JHC, ten Katen HJ, van Es GA, Hugenholtz PG. Incidence of restenosis after successful coronary angioplasty: a time-related phenomenon: A quantitative angiographic study in 342 consecutive patients at 1, 2, 3, and 4 months. *Circulation* 77: 361-371 (1988).
80. Serruys PW, Rutsch W, Heyndrickx GR, Danchin N, Mast G, Wijns W, Rensing BJ, Vos J, Stibbe J, for the Coronary Artery Restenosis Prevention on Repeated Thromboxane-Antagonism Study Group (CARPORT). Prevention of restenosis after percutaneous transluminal coronary angioplasty with thromboxane A₂-receptor blockade. A randomized, double-blind, placebo-controlled trial. *Circulation* 84:1568-1580 (1991).
81. Song PS, Tapley KJ. Photochemistry and photobiology of psoralens. *Photochem Photobiol* 29: 1177-1197 (1979).
82. Spears JR, Reyes VP, Wynne J, Fromm BS, Sinofsky EL, Andrus S, Sinclair IN, Hopkins BE, Schwartz L, Aldridge HE, Plokker HWT, Mast EG, Rickards A, Knudtson ML, Sigwart U, Dear WE, Ferguson JJ, Angelini P, Leatherman LL, Safian RD, Jenkins RD, Douglas JS Jr, King SB III. Percutaneous coronary laser balloon angioplasty: Initial results of a multicenter experience. *J Am Coll Cardiol* 16: 293-303 (1990).
83. Sporn LA, Foster TH. Photofrin and light induces microtubule depolymerization in cultured human endothelial cells. *Cancer Res* 52:3443-3448 (1992).
84. Sumpio BE, Banas AJ. Response of cultured aorta smooth muscle cells to pulsatile stretching. *J Surg Res* 44: 696-701 (1988).
85. Sumpio BE, Li G, Deckelbaum LI, Gasparro FP. Inhibition of smooth muscle cell proliferation by visible light-activated psoralen. *Circ Res* 75: 208-213 (1994).

86. Sumpio BE, Phan SM, Gasparro FP, Deckelbaum LI. Control of smooth muscle cell proliferation by psoralen photochemotherapy. *J Vasc Surg* 17: 1010-1016 (1993).
87. Thyberg J, Hedin U, Sjolund M, Palmberg L, Bottger BA. Regulation of differentiated properties and proliferation of arterial smooth muscle cells. *Arteriosclerosis* 10(6):966-990 (1990).
88. Vos JM, Wauthier EL. Differential introduction of DNA damage and repair in mammalian genes transcribed by RNA polymerases I and II. *Mol Cell Biol* 11:2245-52 (1991).
89. Waller BF. The eccentric coronary atherosclerotic plaque: Morphologic observations and clinical relevance. *J Am Coll Cardiol* 6:1100-1101 (1985).
90. Waller BF, Pinkerton CA, Orr CM, Slack JD, Van Tassel JW, Peters T: Restenosis after clinically successful coronary balloon angioplasty: a necropsy study of 20 patients. *J Am Coll Cardiol* 17:58B-70B (1991).
91. Weintraub WS, Boccuzzi SJ, Brown CL III, Cohen CL, Hirsch LJ, King SB III, Alexander RW, and the Lovastatin Restenosis Trial Study Group. Background and methods for the lovastatin restenosis trial after percutaneous transluminal coronary angioplasty. *Am J Cardiol* 70:293-299 (1992).
92. White CW, Knudson M, Schmidt D, Chisholm RJ, Vandormael M, Morton B, Roy L, Khaja F, Reitman M, and the Ticlopidine Study Group. Neither ticlopidine nor aspirin-dipyridamole prevents restenosis post PTCA: Results from a randomized placebo-controlled multicenter trial (abstract). *Circulation* 76 (Suppl. IV):213 (1987).
93. Whitworth HB, Roubin GS, Hollman J, Meier B, Leimgruber PP, Douglas JS Jr, King SB III, Gruentzig AR. Effect of nifedipine on recurrent stenosis after percutaneous transluminal coronary angioplasty: A randomized study. *J Am Coll Cardiol* 8:1271-1276 (1986).
94. Wilcox JN. Molecular biology: Insight into the causes and prevention of restenosis after arterial intervention. *Am J Cardiol* 72:88E-95E (1993).
95. Wilensky RL, March KL, Hathaway DR. Direct intraarterial wall injection of microparticles via a catheter: A potential drug delivery strategy following angioplasty. *Am Heart J* 122: 1136-1140 (1991).
96. Wilentz JR, Sanborn TA, Haudenschild CC, Valeri CR, Ryan TJ, Faxon DP. Platelet accumulation in experimental angioplasty: time course and relation to vascular injury. *Circulation* 75:636-642 (1991).
97. Yabe Y, Okamoto K, Oosawa H, Miyairi M, Noike H, Aihara M, Muramatu T. Does a thromboxane A2 synthetase inhibitor prevent restenosis after PTCA? (abstract) *Circulation* 80 (Suppl. II):260 (1989).
98. Yang XY, Gasparro FP, DeLeo VA, Santella RM. 8-Methoxypsoralen-DNA adducts in patients treated with 8-methoxypsoralen and ultraviolet A light. *J Inv Derm* 92: 59-63 (1989).



3 9002 08676 0148

HARVEY CUSHING / JOHN HAY WHITNEY
MEDICAL LIBRARY

MANUSCRIPT THESES

Unpublished theses submitted for the Master's and Doctor's degrees and deposited in the Medical Library are to be used only with due regard to the rights of the authors. Bibliographical references may be noted, but passages must not be copied without permission of the authors, and without proper credit being given in subsequent written or published work.

This thesis by _____ has been
used by the following persons, whose signatures attest their acceptance of the
above restrictions.

NAME AND ADDRESS

DATE

